Journal of Medicinal Chemistry

ARTICLE

pubs.acs.org/jmc

Cell-Permeable and Plasma-Stable Peptidomimetic Inhibitors of the Postsynaptic Density-95/*N*-Methyl-D-Aspartate Receptor Interaction

Anders Bach,[†] Jonas N. N. Eildal,[†] Nicolai Stuhr-Hansen, Rasmus Deeskamp, Marie Gottschalk, Søren W. Pedersen, Anders S. Kristensen, and Kristian Strømgaard*

Department of Medicinal Chemistry, The Faculty of Pharmaceutical Sciences, University of Copenhagen, Universitetsparken 2, DK-2100 Copenhagen, Denmark

Supporting Information

ABSTRACT: The protein−protein interaction between the NMDA receptor and its intracellular scaffolding protein, PSD-95, is a potential target for treating ischemic brain diseases, neuropathic pain, and Alzheimer's disease. We have previously demonstrated that *N*-alkylated tetrapeptides are potent inhibitors of this interaction, and here, this template is exploited for the development of blood plasma-stable and cell-permeable inhibitors. Initially, we explored both the amino acid sequence of the tetrapeptide and the nature of the *N*-alkyl groups, which consolidated *N*-cyclohexylethyl-ETAV (**1**) as the most potent and selective compound. Next, the amide moieties of *N*-methylated ETAV were systematically replaced with thioamides, demonstrating that one of three amide bonds could be replaced without compromising the affinity. Subsequent optimization of the *N*-alkyl groups and evaluation of cell permeability led to identification of *N*-cyclohexylethyl-ETA$_S$V (**54**) as the most potent, plasma-stable and cell-permeable inhibitor, which is a promising tool in unraveling the therapeutic potential of the PSD-95/NMDA receptor interaction.

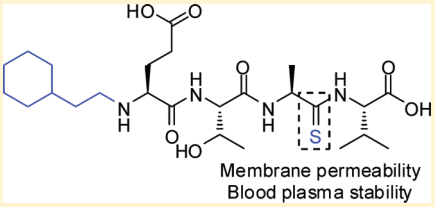

INTRODUCTION

Protein−protein interactions (PPIs) are vital for almost all cellular and biochemical processes and constitute novel and promising targets for the treatment of a range of diseases. Moreover, inhibitors of PPIs are important pharmacological tools for studying biological phenomena.[1,2] The PSD-95/discs-large/ZO-1 (PDZ) protein domain family facilitates several vital PPIs, which are putative targets in the development of drugs for the treatment of cancer and disorders in the central nervous system (CNS).[3−7] PDZ domains are relatively small (∼90 amino acids), typically bind the extreme C-terminal of their protein partner,[8,9] and are highly abundant in the human proteome. They are often found in multidomain scaffold and anchoring proteins involved in trafficking, recruiting, and assembling of intracellular enzymes and membrane receptors into signaling−transduction complexes. PDZ domains increase the specificity and efficiency of intracellular communication networks downstream of receptor activation by facilitating important PPIs between signaling enzymes and receptors.[10,11]

The *N*-methyl-D-aspartate (NMDA) receptor, a subclass of the ionotropic glutamate receptors, is involved in neurological disorders such as neuropathic pain, ischemic stroke, and chronic neurodegenerative diseases such as Alzheimer's disease, where glutamate-mediated overstimulation of the NMDA receptor, known as excitotoxicity, plays a pathophysiological role.[4,12] Upon activation of the NMDA receptor, Ca^{2+} enters the cell through the NMDA receptor ion channel and activates the intracellular enzyme neuronal nitric oxide synthase (nNOS), leading to generation of nitric oxide (NO). NO acts as an important secondary messenger under normal physiological conditions, but excessive activation of the NMDA receptor leads to toxic levels of NO, which contributes to excitotoxicity-mediated neuronal damage.[13,14] Thus, inhibition of the NMDA receptor has been extensively pursued as a potential neuroprotective strategy. However, clinical development of antagonists that bind directly to the NMDA receptor has proven difficult due to severe side effects such as psychosis and memory impairment.[4,12,15,16]

Instead of modulating NMDA receptor activity directly, an alternative approach is to uncouple the PPI between the intracellular scaffolding protein postsynaptic density protein-95 (PSD-95) and the NMDA receptor. PSD-95 bridges the NMDA receptor and nNOS via PDZ domains,[17] and it has been demonstrated that inhibition of the PSD-95/NMDA receptor interaction reduces NMDA-mediated NO production and prevents excitotoxic insults in cultured neurons and ischemic brain damage in vivo.[18,19] In addition, it has recently been shown that uncoupling of the PSD-95/NMDA receptor interaction might also have therapeutic potential in neuropathic pain and in Alzheimer's disease.[20−23] Because this strategy does not affect the ion channel function of the NMDA receptor that is required for normal excitatory neurotransmission, the side effects observed for conventional NMDA receptor antagonists may be avoided. Inhibiting the PSD-95/NMDA receptor interaction therefore comprises a promising strategy for the development of neuroprotective drugs.

PSD-95 contains three sequential PDZ domains, PDZ1−3, which bind peptide ligands containing the consensus sequence

Received: October 26, 2010
Published: February 15, 2011

dx.doi.org/10.1021/jm1013924 | *J. Med. Chem.* 2011, 54, 1333–1346

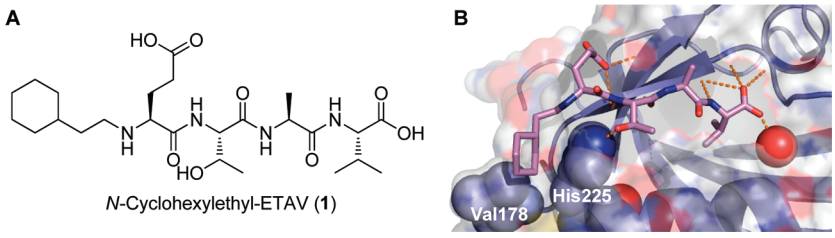

Figure 1. (A) Structure of **1**. (B) Compound **1** docked into the PDZ2 homology model.[28] Compound **1** is shown with sticks using purple carbons, red oxygens, and blue nitrogens. The PDZ2 domain is shown as a blue cartoon model, with an indication of its electron surface, where carbons are shown in white, oxygens in red, and nitrogens in blue. The red sphere (to the right) indicates a water molecule. Hydrogen bonds and electrostatic interactions are indicated with orange dashes, and PDZ residues discussed in the text are highlighted.

Glu/Gln-Ser/Thr-X-Val-COOH. PDZ1 and PDZ2 display the same selectivity profile against a broad range of peptide ligands and interact with the C-terminal tail of the NMDA receptor subunits (GluN2A-D),[24−26] with an in vitro affinity for GluN2B of 18 and 4 μM for PDZ1 and PDZ2, respectively.[27,28] Generally, it has been exceedingly difficult to identify small molecule inhibitors of PDZ domains with reasonable potency (K_i < 10 μM),[29] which can be rationalized by a shallow and elongated binding pocket of PDZ domains that is more suited for peptide-based ligands.[30,31] Thus, to this date, potent inhibitors of the PDZ domains of PSD-95 have only been identified by peptide-based strategies,[32−35] which include side chain cyclization of a hexapeptide[32] and dimerization of peptide ligands.[35] However, the most advanced PDZ domain inhibitor in terms of drug development is a 20-mer linear peptide Tat-N2B (NA-1, YGRKKRRQRRR-KLSSIESDV),[18] which is currently undergoing clinical phase II trials as a potential neuroprotective drug related to stroke and endovascular procedures.[36] Although possessing only modest affinity toward PSD-95 (K_i ∼ 4.4 μM against PDZ2), Tat-N2B displays neuroprotective efficacy in cultured neurons and in in vivo stroke models.[18,19,28]

Recently, we have exploited the C-terminal tail of the GluN2B subunit (YEKLSSIESDV) as a template for development of inhibitors of the PSD-95/NMDA receptor interaction with reduced size and increased potency.[28] First, we demonstrated that the C-terminal pentapeptide (IESDV) displayed wild-type affinity, while tetra- and tripeptides showed a stepwise reduction in affinities. Second, we observed that N-alkylation of tetrapeptides enhanced affinity up to 40-fold and identified *N*-cyclohexylethyl ETAV (**1**) as a potent inhibitor of PDZ2 of PSD-95 with a K_i of 0.5 μM (Figure 1), representing an almost 10-fold increase in potency as compared to the wild-type GluN2B C-terminal tail.[28]

Here, we have elaborated on N-alkylated tetrapeptides as inhibitors of the PSD-95/NMDA receptor interaction, focusing on optimizing compound stability in blood plasma and cell membrane permeability. Initially, we performed a structure−activity relationship (SAR) study where combinations of tetrapeptides and *N*-alkyl groups were prepared and investigated for their potency and selectivity. Subsequently, a range of structurally diverse *N*-alkyl groups were introduced in the ETAV tetrapeptide. We next explored the possibility of replacing amide bonds with thioamides, which resulted in compounds with complete stability in human blood plasma in vitro, while affinity was preserved. Finally, the optimized compounds were investigated in a cell-based bioluminescence resonance energy transfer (BRET) assay, demonstrating their ability to penetrate cell membranes and inhibit the PSD-95/NMDA receptor interaction in living cells.

RESULTS AND DISCUSSION

N-Alkylated tetrapeptides were recently identified as potent inhibitors of the PSD-95/NMDA receptor interaction.[28] However, only a limited number of tetrapeptide sequences and *N*-alkyl groups were investigated; thus, a more thorough SAR study of these tetrapeptide derivatives aiming at optimizing affinity toward PDZ2 of PSD-95, as well as preserving selectivity relative to PDZ3, was warranted.

It is generally acknowledged that amino acids in position P^0 and P^{-2} (counting from the C-terminal amino acid) are key determinants for affinity.[24,26,27] In agreement with this, we found that Val in P^0 and Ser or Thr in P^{-2} were crucial for affinity to PDZ1 and PDZ2 of PSD-95, and we showed that Glu in the P^{-3} position was important for affinity, whereas Asp in P^{-1} could be replaced with Ala or Gln without substantial loss in affinity.[28] On the basis of these results, a series of tetrapeptides and their corresponding N-alkylated tetrapeptides, **1**−**12**, were designed (Table 1). The compounds were prepared by standard Fmoc-based solid-phase peptide synthesis (SPPS) followed by N-alkylation using the Fukuyama−Mitsunobu reaction, and their affinities toward PDZ2 and PDZ3 of PSD-95 were measured in our well-established fluorescence polarization (FP) assay.[28] Generally, it was found that substituting Asp in P^{-1} with Ala reduces affinity toward PDZ2 less than 3-fold, and in the case of compound **1**, equal affinity was seen as compared to **8** (Table 1). Substituting Glu in P^{-3} generally led to larger decreases in affinity; however, Ala was better tolerated than Gln (Table 1).

Because the wild-type undecapeptide sequence of GluN2B (YEKLSSIESDV) possesses no affinity toward PDZ3, which instead binds to the C-terminal of cysteine-rich PDZ-binding protein (CRIPT, LDTKNYKQTSV),[28,37] the relationship between the K_i values of PDZ3 and PDZ2 is used as a measure of selectivity. It is apparent that the *N*-alkyl group and the amino acid in the P^{-3} position do not affect the selectivity for PDZ2, which is almost entirely determined by the amino acid in the P^{-1} position (Table 1). Thus, selectivity is achieved with Asp in P^{-1} (compounds **3**, **5**, **7**, **8**, **10**, and **12**; Table 1), whereas Ala in the same position entails increased binding to PDZ3, although 10−20-fold selectivity for PDZ2 is still observed.

To investigate if these findings were valid for *N*-alkyl groups other than cyclohexylethyl, a smaller series of six compounds (**13**−**18**) were prepared where either (naphthalene-2-yl)ethyl or (3,4-dichlorophenyl)ethyl were introduced into the N-terminal amino group of three different tetrapeptides (Table 1). In agreement with the cyclohexylethyl N-alkylated compounds, substitutions in the P^{-3} position led to the most dramatic decreases in affinity, whereas the P^{-1} position is the major determinant of

Table 1. K_i Values of *N*-Alkylated Tetrapeptides with the General Structure

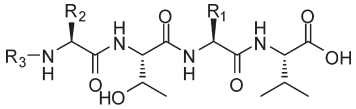

R_1 = CH_3 (Ala) or CH_2COOH (Asp)
R_2 = CH_3 (Ala), CH_2CH_2COOH (Glu), or $CH_2CH_2CONH_2$ (Gln)

compound	sequence	R_3	PDZ2[a]	PDZ3[a]	selectivity[b]
GluN2B[d]	YEKLSSIESDV		4.1 ± 0.17	NA[c]	>1000
CRIPT [d]	LDTKNYKQTSV		25 ± 1.6	2.1 ± 0.15	0.08
1	ETAV	cyclohexylethyl	0.63 ± 0.055	11 ± 0.79	17
2[d]	ETAV	H	22 ± 0.92	260 ± 20	12
3[d]	ETDV	H	16 ± 0.88	NA	>1000
4	QTAV	H	110 ± 6.3	>400	>4
5	QTDV	H	60 ± 1.9	NA	>1000
6	ATAV	H	73 ± 3.8	>400	>4
7	ATDV	H	38 ± 4.2	NA	>1000
8	ETDV	cyclohexylethyl	0.75 ± 0.13	NA	>1000
9	QTAV	cyclohexylethyl	12 ± 0.36	141 ± 14	12
10	QTDV	cyclohexylethyl	4.4 ± 0.59	NA	>1000
11	ATAV	cyclohexylethyl	8.1 ± 0.12	89 ± 3.3	11
12	ATDV	cyclohexylethyl	3.6 ± 0.30	>400	>110
13[d]	ETAV	(naphthalene-2-yl)ethyl	0.95 ± 0.05	10 ± 0.22	11
14[d]	ETAV	(3,4-dichlorophenyl)ethyl	1.1 ± 0.11	6.7 ± 0.20	6
15	ETDV	(naphthalene-2-yl)ethyl	1.8 ± 0.15	210 ± 8.5	117
16	ETDV	(3,4-dichlorophenyl)ethyl	1.2 ± 0.049	130 ± 3.4	109
17	ATAV	(naphthalene-2-yl)ethyl	56 ± 1.8	280 ± 9.0	5
18	ATAV	(3,4-dichlorophenyl)ethyl	13 ± 1.1	64 ± 2.4	5

[a] K_i values are shown as means ± SEMs in μM based on at least three individual measurements. [b] K_i (PDZ3)/K_i (PDZ2). [c] NA, no affinity. [d] Data from ref 28.

selectivity. Finally, it is apparent that the *N*-cyclohexylethyl group led to the largest increase in affinity regardless of the sequence of the tetrapeptide (Table 1). On the basis of these results, the ETAV sequence was chosen for further optimization of the *N*-alkyl group, as ETAV offers the most favorable balance between affinity, selectivity, and physical properties such as polarity and size.

Docking of *N*-cyclohexylethyl-ETAV (**1**) into a homology model of PDZ2 (Figure 1B)[28] suggested that the *N*-alkyl group binds in a small hydrophobic cavity created by Val178 and His225 from the βB−βC loop and the αB helix, respectively, of PDZ2. When the pentapeptide IESDV is docked into PDZ2, this cavity is occupied by the side chain of Ile.[28] To investigate if this hydrophobic cavity is fully exploited by the *N*-cyclohexylethyl group of **1**, we tested the effect of introducing larger and more hydrophobic *N*-alkyl substituents.

A series of 12 *N*-alkyl groups were selected with variation in bulkiness and hydrophobicity. The alcohols required for N-alkylation were acquired from commercial sources, obtained by reduction of the corresponding carboxylic acids or synthesized from closely related starting materials (Supporting Information). These alcohols were subsequently used in the Fukuyama−Mitsunobu reaction to alkylate the N terminus of ETAV to furnish compounds **19**−**30** (Table 2). Evaluation in the FP assay revealed that most of the derivatives displayed increased affinity toward PDZ2 as compared to non-alkylated tetrapeptide ETAV (**2**), and several compounds had K_i values around 1−2 μM. However, none of them showed improved affinity or selectivity relative to *N*-cyclohexylethyl-ETAV (**1**). Compounds **24**−**30** were designed based upon *N*-(3,4-difluorophenyl)ethyl-ETAV and *N*-(naphthalene-2-yl)ethyl-ETAV (**13**) having K_i values of 1.0 and 0.95 μM, respectively. However, increasing the length or the number of fluorine substituents on the phenyl ring reduced affinity (**24** and **25**, Table 2) and similarly increasing the alkyl chain length or the size of the aromatic moiety also reduced affinity (**26**−**30**, Table 2). Thus, the ETAV tetrapeptide sequence combined with an *N*-cyclohexylethyl substituent as in **1** is the most potent and selective compound of the series.

One of the primary limitations for advanced biological studies of peptide-based compounds is their low stability in blood and tissues due to enzymatic cleavage by proteases or peptidases, which efficiently hydrolyze the amide bonds. Several strategies have been pursued to increase stability for PDZ peptide ligands for example by derivatization of the N terminus with a short polyethylene glycol (PEG) linker[35] or by introducing a conformationally restricted central amino acid in a tripeptide.[33] Also, cyclization of the P^{-1} and P^{-3} amino acid side chains increased the duration of activity in a cell-based assay.[32]

We considered replacing the amide bonds of **1** with thioamides as a general and straightforward way of obtaining increased stability in human blood plasma without modifying the peptide side chains and thereby impairing affinity or selectivity, as also demonstrated for other peptides.[38−43] Thioamides generally

dx.doi.org/10.1021/jm1013924 |J. Med. Chem. 2011, 54, 1333–1346

Table 2. K_i Values of *N*-Alkylated ETAV Peptides

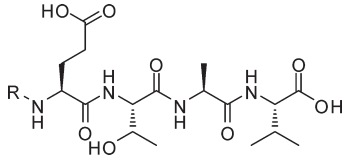

Compound	R	PDZ2[a]	PDZ3[a]	Selectivity[b]
2[c]	H	22 ± 0.92	260 ± 20	12
1	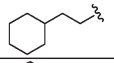	0.63 ± 0.055	11 ± 0.79	17
19	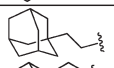	2.1 ± 0.30	6.7 ± 0.42	3
20	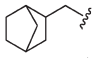	1.3 ± 0.064	20 ± 2.2	16
21	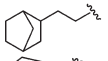	1.5 ± 0.18	14 ± 0.46	9
22	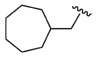	1.4 ± 0.12	16 ± 0.75	12
23	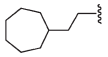	1.2 ± 0.11	9.4 ± 0.26	8
24	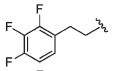	1.8 ± 0.23	8.8 ± 0.63	5
25	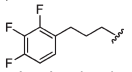	4.2 ± 0.74	44 ± 3.1	10
26	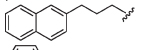	5.0 ± 0.43	53 ± 4.0	11
27	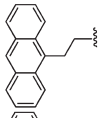	9.7 ± 0.43	3.9 ± 0.24	0.4
28	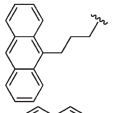	9.0 ± 0.12	95 ± 2.5	11
29	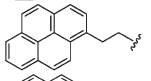	16 ± 1.7	51 ± 4.3	3
30	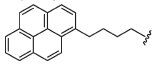	33 ± 0.67	76 ± 4.9	2

[a] K_i values are shown as means ± SEMs in μM based on at least three individual measurements. [b] K_i (PDZ3)/K_i (PDZ2). [c] Data from ref 28.

mimic amides, but increased rigidity is introduced as the larger sulfur atom and longer carbon−sulfur bond restrict φ and ψ angles.[44] Moreover, thioamides have increased hydrophobicity, and the thiocarbonyl is a weaker hydrogen bond acceptor than the carbonyl oxygen.[38,45] Thus, initially each of the three amide bonds in *N*-methylated ETAV (*N*-Me-ETAV, **31**) were substituted with a thioamide functionality, and the thioamide derivatives were evaluated for affinity toward PDZ2.

The Lawesson's reagent was selected as a mild and convenient way to convert amides into thioamides.[46,47] Initial attempts to perform the thionation on the solid phase failed; therefore, protected dipeptides were treated with Lawesson's reagent in solution. For each of the three thioamide derivatives, compounds **35**, **41**, and **45**, different synthetic strategies were required. For compound **35**, where the amide bond between residues P^0 and P^{-1} is replaced with a thioamide, the protected dipeptide Fmoc-Ala-Val-O-*tert*-Bu (**32**) was prepared and subsequently converted into the corresponding thioamide **33** by treatment with Lawesson's reagent in THF for 24 h (Scheme 1). Treating **33** with trifluoroacetic acid (TFA) provided **34**, which was loaded to a 2-chlorotrityl chloride resin, and standard SPPS provided the desired compound *N*-Me-ETA$_S$V (**35**, Scheme 1).

In a similar manner, the amide bond between the P^{-1} and the P^{-2} residues was converted into a thioamide. The protected dipeptide, Fmoc-Thr(O-*tert*-Bu)-Ala-O-*tert*-Bu (**36**), was treated with Lawesson's reagent and converted into a thioamide to furnish **37** (Scheme 2). Subsequently, **37** was treated with TFA to give deprotected dipeptide **38**, which was coupled to Val-O-*tert*-Bu in solution providing **39**. Removal of the Fmoc protecting group with dimethylamine, followed by coupling with Fmoc-*N*-Me-Glu(O-*tert*-Bu)-OH provided **40**, and deprotection gave *N*-Me-ET$_S$AV (**41**, Scheme 2).

Introduction of the thioamide between the P^{-2} and the P^{-3} amino acids was more challenging and required an orthogonal protecting group strategy for the two carboxylic acid groups in the protected dipeptide **43** (Scheme 3). Initially, Fmoc-Thr-(O-*tert*-Bu)-OH was loaded on to a 2-chlorotrityl chloride resin followed by Fmoc deprotection and subsequent coupling with Fmoc-*N*-Me-Glu(O-*tert*-Bu)-OH. Treatment of this resin with hexafluoroisopropanol (HFIP)[48] provided the protected dipeptide **42**, which allowed a selective protection of the C-terminal carboxylic acid with *tert*-butyldiphenylsilyl (TBDPS) chloride to give **43** (Scheme 3). This dipeptide was treated with Lawesson's reagent providing **44**, and subsequent removal of the TBDPS group with tetrabutylammonium fluoride (TBAF) allowed coupling to resin-bound H-Ala-Val. Finally, Fmoc deprotection and TFA cleavage provided the target compound *N*-Me-E$_S$TAV (**45**, Scheme 3).

Compounds **35**, **41**, and **45** were tested for affinity to PDZ2 and PDZ3, as well as for their stability in human blood plasma, using *N*-Me-ETAV (**31**) as a reference compound. Interestingly, the three compounds demonstrated very different properties both in affinity and in stability: Compound **35**, containing a thioamide between the P^0 and the P^{-1} residues, was equipotent to **31** and displayed complete stability in plasma as measured over 5500 min (~92 h, Figure 2). In contrast, **41** having the thioamide placed between the P^{-1} and the P^{-2} residues showed a considerable loss (23-fold) in affinity toward PDZ2. The stability of **41** in blood plasma was improved as compared to **31** with $T_{1/2}$ = 540 ± 50 min but significantly less than **35**. Finally, **45** with the thioamide between the P^{-2} and the P^{-3} residues also demonstrated complete stability in plasma, but affinity was reduced by 3.3-fold as compared to **31** (Figure 2). For all three compounds, PDZ2 vs PDZ3 selectivity was not affected by the introduction of thioamides (data not shown). Thus, gratifyingly, a thioamide can be introduced instead of the amide bond between residues P^0 and P^{-1} as in **35** without compromising biological activity, whereas complete stability in blood plasma is achieved.

To rationalize the biological activity in a structural context, compound **31** and the thioamide derivatives **35**, **41**, and **45** were docked into a homology model of PDZ2, which is based on the X-ray crystal structure of PDZ3 in complex with the C-terminal peptide from CRIPT.[28,37] Docking of **31** showed that the backbone superimposes with the CRIPT peptide in PDZ3, and similar to the CRIPT-PDZ3 interaction, the amide carbonyl group of Thr (P^{-2}) in **31** forms a hydrogen bond with a backbone amide hydrogen from PDZ2 (Figure 3A). Because the thiocarbonyl sulfur is a weaker hydrogen bond acceptor than the carbonyl oxygen, it is not surprising that a substantial loss in affinity is seen when the P^{-2} amide carbonyl is replaced with thiocarbonyl as in **41**. In contrast, the amide carbonyl groups from the P^{-1} and P^{-3} positions do not have any direct interactions with the PDZ domain (Figure 3A),

Scheme 1[a]

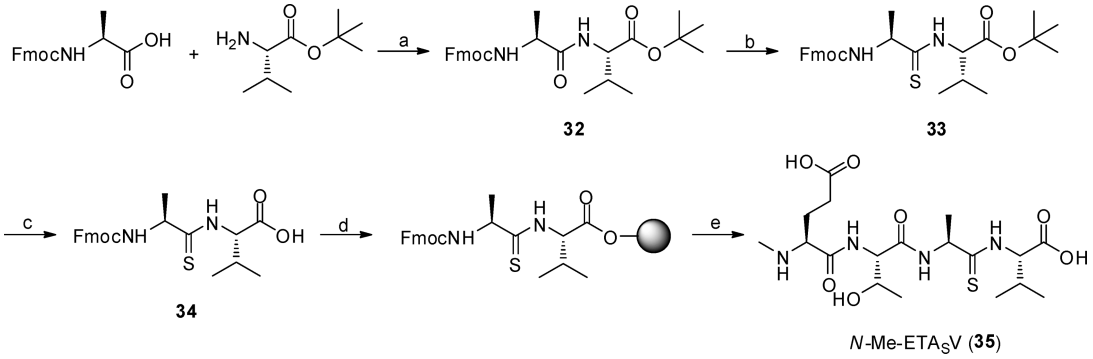

[a] Reagents and conditions: (a) HBTU, Et_3N, MeCN. (b) Lawesson's reagent, THF. (c) TFA, DCM. (d) 2-Chlorotrityl chloride resin, DIPEA, DCM. (e) (i) 30% piperidine in DMF; (ii) Fmoc-Thr(O-*tert*-Bu)-OH, HBTU, DIPEA, DMF; (iii) 30% piperidine, DMF; (iv) Fmoc-*N*-Me-Glu(O-*tert*-Bu)-OH, HBTU, DIPEA, DMF; (v) 30% piperidine in DMF; (vi) TFA, TIPS, H_2O (90:5:5).

Scheme 2[a]

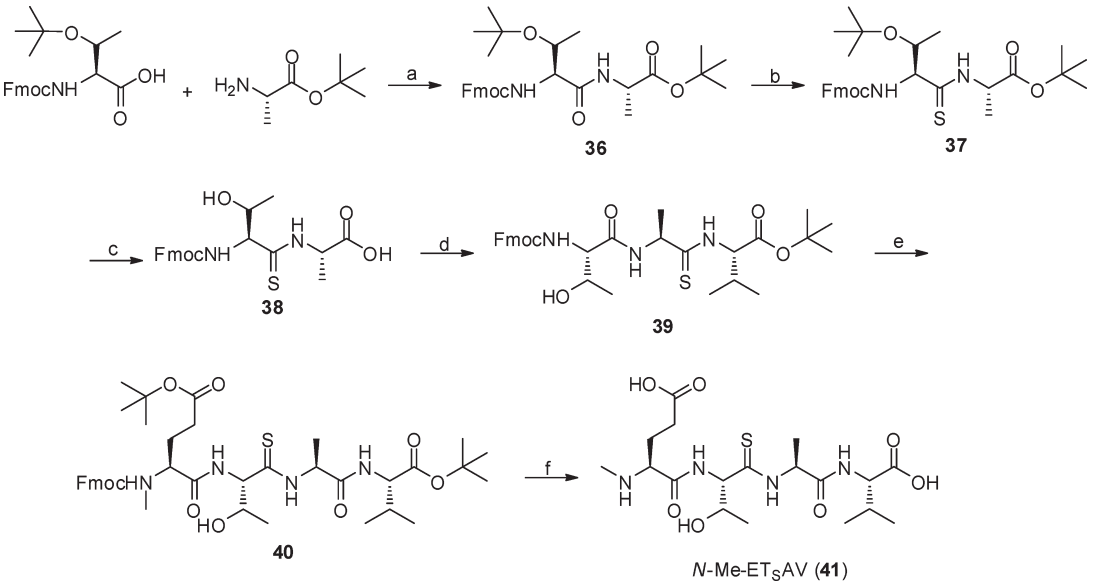

[a] Reagents and conditions: (a) HBTU, Et_3N, MeCN. (b) Lawesson's reagent, THF. (c) TFA, DCM. (d) H-Val-O-*tert*-Bu, HBTU, DIPEA, DMF. (e) (i) Me_2NH, MeOH; (ii) Fmoc-*N*-Me-Glu(O-*tert*-Bu)-OH, HBTU, DIPEA, DMF. (f) (i) Me_2NH, MeOH; (ii) TFA, TIPS, H_2O (90:5:5).

explaining that thioamides in these positions do not affect affinity to PDZ2 to a great extent. Docking of compounds **35**, **41**, and **45** into PDZ2 reveals that **35** binds to PDZ2 in the same conformation as **31** (Figure 3B), whereas a twist in the backbone region around P^{-3} position is seen for **41** and **45**. Moreover, the positioning of the Glu and Thr side chains of **41** and **45** deviates from that of **31**. These results suggest that thioamides **35**, **41**, and **45** generally bind in a manner similar to that of **31** but that minor differences are observed for **41** and **45**, which lead to reduced affinities (Figure 3B).

Encouraged by the results of the thioamide derivatives, we next aimed at combining high affinity and selectivity, low polarity, and high blood plasma stability into one compound. Thus, we hypothesized that introduction of a thioamide between the P^0 and the P^{-1} residue of ETAV, combined with the *N*-alkyl groups, *N*-cyclohexylethyl, *N*-(naphthalene-2-yl)ethyl, or *N*-(3,4-dichlorophenyl)ethyl, could provide compounds with the desired properties. Initially, a linear synthetic route was attempted, and dipeptide Fmoc-A_SV-OH (**34**) was loaded on a 2-chlorotrityl chloride resin, followed by SPPS to obtain the thioamide-tetrapeptide ETA_SV. However, the conditions for the Fukuyama−Mitsunobu synthesis (Ph_3P and DIAD) were not compatible with the thioamide moiety, as the desired N-alkylated product could not be identified. Instead, a convergent approach was attempted, where Fmoc-Glu(O-*tert*-Bu)-OH was loaded to the resin to give **46**, and after Fmoc deprotection and introduction of the 2-nitrobenzenesulfonyl (Ns) group, the N-terminal sulfonamide was alkylated using the Fukuyama−Mitsunobu method to provide **47**−**49** (Scheme 4). The N-alkylated Glu derivatives were subsequently cleaved from the resin by treatment with HFIP to furnish the appropriately protected N-alkylated amino acids (**50**−**52**, Scheme 4). In parallel, **34** was loaded on a 2-chlorotrityl chloride resin and Fmoc deprotected, followed by coupling with Fmoc-Thr(O-*tert*-Bu)-OH and removal of the Fmoc group (**53**). Subsequent coupling of **50**−**52** to **53**, removal of the Ns group, and TFA cleavage provided the target compounds **54**−**56** (Scheme 4). In contrast to the N-methylated thioamide derivatives **35**, **41**, and **45**, some epimerization (15−25%) was observed in the

dx.doi.org/10.1021/jm1013924 |*J. Med. Chem.* 2011, 54, 1333–1346

Scheme 3[a]

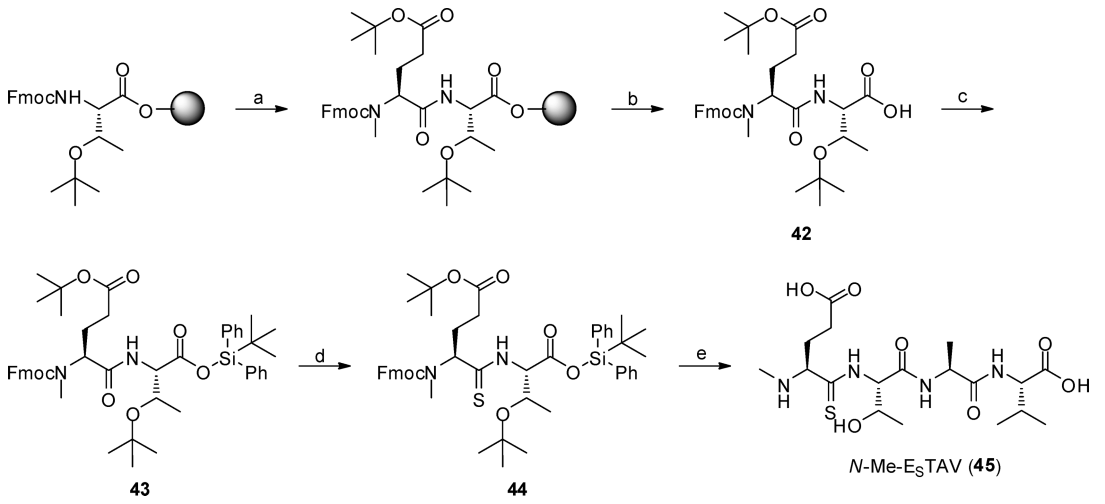

[a] Reagents and conditions: (a) (i) 30% piperidine in DMF; (ii) Fmoc-*N*-Me-Glu(O-*tert*-Bu)-OH, HBTU, DIPEA, DMF. (b) HFIP, DCM. (c) TBDPS, DIPEA, DMF. (d) Lawesson's reagent, THF. (e) (i) TBAF, THF; (ii) H-Ala-Val-(2-chlorotrityl resin), HBTU, DIPEA, DMF; (iii) 30% piperidine in DMF; (iv) TFA, TIPS, H_2O (90:5:5).

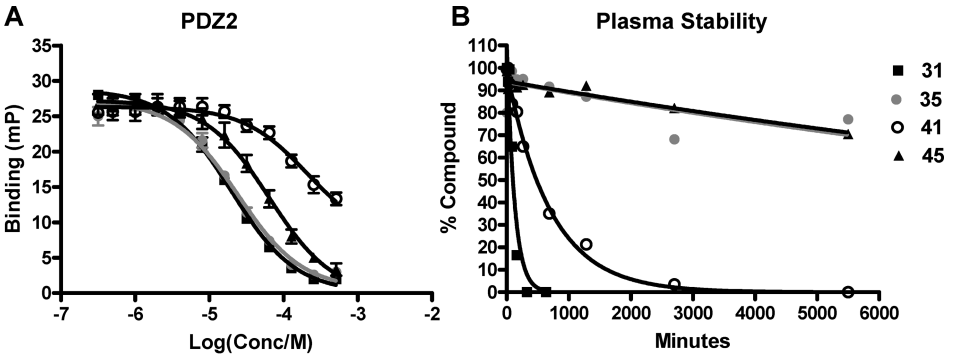

C

Compound	Structure	PDZ2 (K_i/μM)	Stability ($T_{1/2}$/min)
31	*N*-Me-ETAV	9.65 ± 0.50	113 ± 9
35	*N*-Me-ETA$_S$V	10.8 ± 0.36	>5500
41	*N*-Me-ET$_S$AV	220 ± 11	540 ± 50
45	*N*-Me-E$_S$TAV	32 ± 2.8	>5500

Figure 2. Biological properties of **31**, **35**, **41**, and **45**. (A) FP affinitiy measurements between compounds and PDZ2 of PSD-95. (B) Stability of compounds in human blood plasma. (C) Table of K_i values (μM) shown as means ± SEMs, based on at least three individual experiments in the FP assay, and plasma half-lives ($T_{1/2}$) in minutes in human blood plasma shown as means ± SEMs, based on at least two individual experiments.

synthesis of **54**−**56** as indicated by HPLC and NMR. However, the diastereomers were separated by preparative HPLC, and the desired isomer was obtained in >95% diastereomeric excess.

Gratifyingly, the N-alkylated thioamide derivatives **54**−**56** were equipotent to their corresponding amide derivatives **1**, **13**, and **14**, respectively (Table 3), with the *N*-cyclohexylethyl derivative (**54**) being the most potent. In addition, the three N-alkylated thioamide derivatives showed complete stability in human blood plasma within the period of measurement (117 h) in contrast to the corresponding nonthioamide containing compounds (Table 3). This substantiates that the observed increase in blood plasma stability is mediated by the introduction of the thioamide only and is independent of the nature of the *N*-alkyl group (Table 3).

The PSD-95/NMDA receptor interaction is located intracellularly, and a prerequisite for these compounds to be used in further biological studies is therefore that they can permeate cell membranes and uncouple the interaction within an intracellular environment. To address both membrane permeability and inhibitory effect in living cells, we have developed a cell-based BRET assay.[49] In this assay, fusion proteins, where the C-terminal of the NMDA receptor subunit GluN2B is fused to green fluorescent protein (GFP) and the PDZ2 domain of PSD-95 is fused to Renilla luciferase (Rluc), are expressed in COS-7 cells. Interaction between the GluN2B terminal and the PDZ2 brings GFP and Rluc together and enables a BRET signal to be detected.[49]

dx.doi.org/10.1021/jm1013924 |*J. Med. Chem.* 2011, 54, 1333–1346

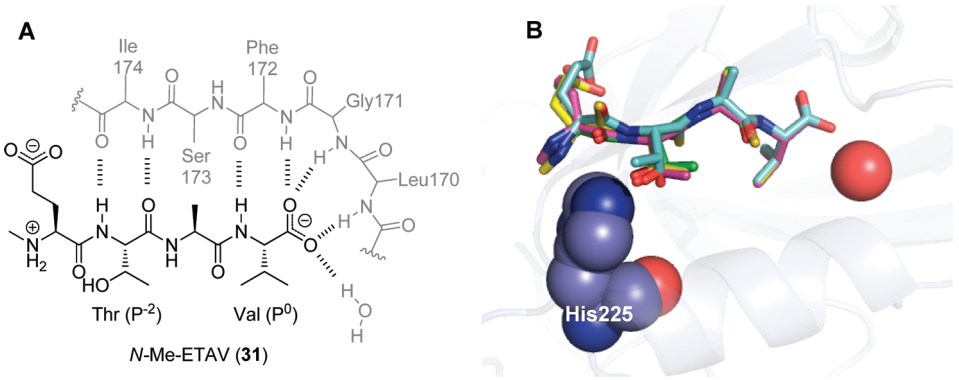

Figure 3. Docking studies of compounds **31**, **35**, **41**, and **45** into the PDZ2 homology model. (A) Schematic representation of the contacts between **31** (black) and backbone amides of PDZ2 (gray) of PSD-95. Dashed lines represent hydrogen bonds. (B) Binding conformations of **31** (green carbons), **35** (purple carbons), **41** (turquoise carbons), and **45** (yellow carbons) in the PDZ2 binding pocket. Oxygens are shown in red, and nitrogens are shown in blue.

Scheme 4[a]

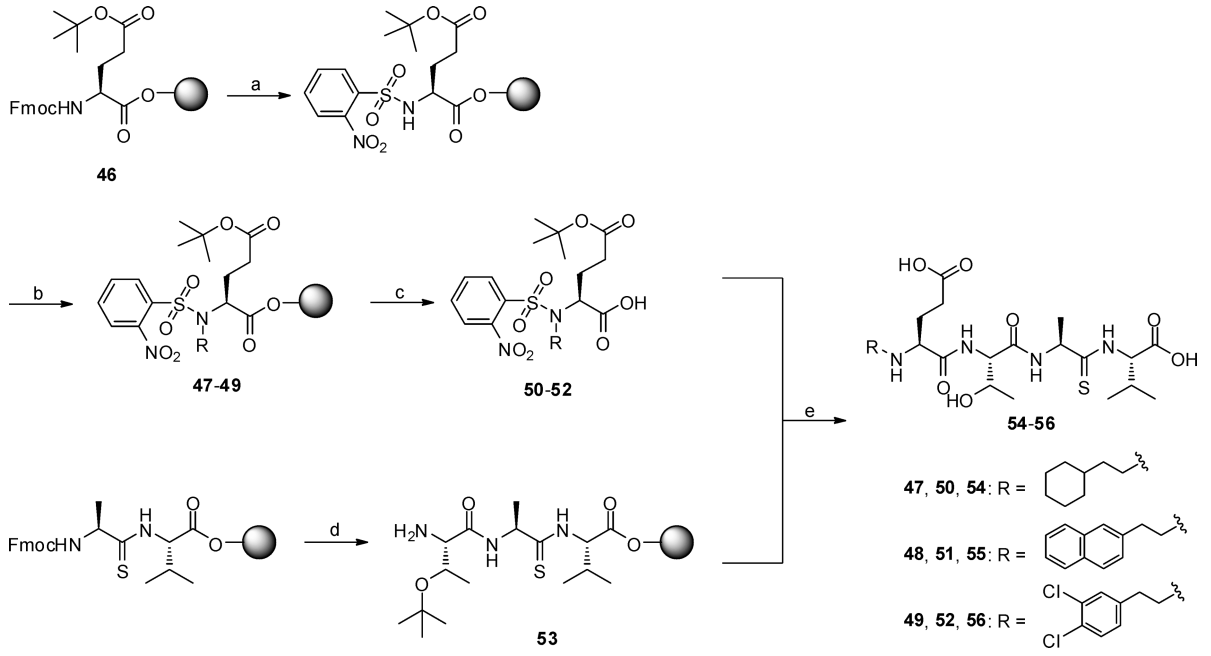

[a] Reagents and conditions: (a) (i) 20% piperidine in DMF; (ii) *o*-Nitrobenzenesulfonyl chloride, DIPEA, THF/DCM. (b) Ph_3P, R-OH, DIAD. (c) HFIP, DCM. (d) (i) 20% piperidine in DMF; (ii) Fmoc-Thr(O-*tert*-Bu)-OH, HBTU, DIPEA, DMF; (iii) 20% piperidine, DMF. (e) (i) HATU, HOAt, collidine; (ii) DBU, mercaptoethanol, DMF; (iii) TFA, TIPS, H_2O (90:5:5).

During validation of our BRET assay, we used the Tat-N2B peptide as a positive control to inhibit GluN2B/PDZ2-mediated BRET in COS-7 cells. Although the Tat moiety is frequently utilized as a cell-penetrating peptide (CPP),[50] it has also been reported that this effect is highly dependent on cell type.[51] Thus, to investigate whether other CPPs than Tat could improve cell permeability, four different fluorescently labeled CPPs fused to the N terminus of GluN2B peptide (**57**−**60**) were synthesized, together with fluorescently labeled Tat-N2B (**61**) (Figure 4). Uptake of the peptides into COS-7 cells was characterized by fluorescence microscopy, and a noticeable difference in cell permeability was observed as follows: Peptide **59** with an Arg octapeptide (Arg8) as the CPP moiety was highly efficient in mediating cell permeability, whereas the Tat sequence (**61**) displayed less permeation (Figure 4). This is in agreement with a previous study that directly compared the ability of CPPs to facilitate cell permeability and observed that Arg8 was more efficient than Tat.[50] The three remaining CPP sequences (**57**, **58**, and **60**) did not facilitate detectable membrane permeability in COS-7 cells. In the BRET assay, the 17-mer peptide **62** (Arg8-N2B, RRRR-RRRR-KLSSIESDV) caused a significant inhibition of the BRET signal at 100 μM and was subsequently used as a control compound (Figure 5).

We subsequently screened a range of N-alkylated peptides (**1**, **8**, **11**, **13**−**19**, and **24**), thioamides (**54**−**56**), and the nonmodified tetrapeptides (**2**, **3**, and **6**) in a concentration of 500 μM for the ability to inhibit BRET. It was found that the three optimized N-alkylated thioamide peptides (**54**−**56**) and their corresponding amide derivatives (**1**, **13**, and **14**) significantly inhibited BRET. The polar, but potent, N-alkylated analogues (**8**, **15**, and **16**) and the non-alkylated tetrapeptides (**2**, **3**, and **6**) did not

dx.doi.org/10.1021/jm1013924 |*J. Med. Chem.* 2011, 54, 1333–1346

Table 3. K_i Values of Optimized *N*-Alkylated Thioamide ETAV Peptides

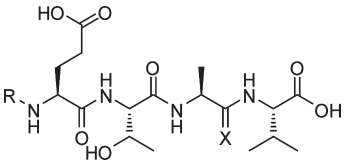

compound	R	X	PDZ2[a]	PDZ3[a]	selectivity[b]	stability ($T_{1/2}$/min)
2[c]	H	O	22 ± 0.92	260 ± 20	12	106 ± 18
1	cyclohexylethyl	O	0.63 ± 0.055	11 ± 0.79	17	29 ± 8
13	(naphthalene-2-yl)ethyl	O	0.95 ± 0.05	10 ± 0.22	11	92 ± 7
14	(3,4-dichlorophenyl)ethyl	O	1.1 ± 0.11	6.7 ± 0.20	6	83 ± 5
54	cyclohexylethyl	S	0.63 ± 0.031	11 ± 0.97	17	>7000
55	(naphthalene-2-yl)ethyl	S	1.1 ± 0.13	11 ± 0.44	10	>7000
56	(3,4-dichlorophenyl)ethyl	S	1.0 ± 0.10	8.3 ± 0.76	8	>7000

[a] K_i values are shown as means ± SEMs in μM based on at least three individual measurements. [b] K_i (PDZ3)/K_i (PDZ2). [c] Data from ref 28.

Figure 4. Cell permeability of fluorescently labeled CPP-N2B peptides in COS-7 cells investigated by fluorescent microscopy. The peptides **57** (*F*-RRRERRAEK-GluN2B), **58** (*F*-KCPSRRPKR-GluN2B), and **60** (*F*-YARAAARQARA-GluN2B) were also tested, but no fluorescence could be detected in the cells. 5-FAM (*F*) alone was tested as a background control. GluN2B: KLSSIESDV.

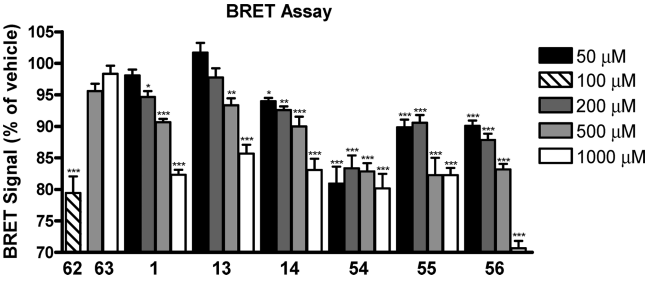

Figure 5. Dose−response relationship of extracellularly applied compounds for inhibition of intracellular BRET in COS-7 cells expressing the GluN2B-GFP terminal and PDZ2-Rluc. BRET signals from cells treated with varying compound concentrations are normalized to the BRET signal from cells treated with vehicle (see the Experimental Section). Values are means ± SEMs from at least three individual experiments. *$p < 0.05$, **$p < 0.01$, and *** $p < 0.001$ significantly different from vehicle; paired Student's *t* test.

demonstrate activity, suggesting that the ETAV peptide sequence in combination with N-alkylation is required for obtaining effect in the BRET assay.

The dose−response relationship of the six active compounds was then tested in the BRET assay at four different concentrations (50, 200, 500, and 1000 μM), and dose dependency was observed for compounds **1**, **13**, **14**, **55**, and **56**, as analyzed by a one-way analysis of variance (ANOVA) including a post test for linear trend ($P < 0.001$) (Figure 5). *N*-(3,4-Dichlorophenyl)-propyl-EAAA (**63**) was included as a negative control, as it is structurally similar to the tested compounds but is devoid of in vitro binding activity at PDZ2 (data not shown). Indeed, **63** did not significantly reduce the BRET signal, verifying that the inhibitory effects observed in the BRET assay are mediated by specific compound interactions with PDZ2 (Figure 5). Furthermore, comparison of thioamides **54**−**56** with their corresponding amide derivatives (**1**, **13**, and **14**) by a two-way ANOVA analysis showed that **54**−**56** are significantly ($P < 0.001$) more potent than **1**, **13**, and **14** in this assay. This improved inhibitory activity in the BRET assay could reflect the increased stability and/or increased membrane permeability of the thioamide compounds.

CONCLUSION

We have explored the N-alkylated tetrapeptide **1** in the search for potent, selective, plasma-stable, and cell-permeable inhibitors of the PSD-95/NMDA receptor interaction, as potential pharmacological tools and therapeutic leads related to stroke, neuropathic pain, and Alzheimer's disease. Initially, a systematic SAR study was carried out, where combinations of tetrapeptide sequences and *N*-alkyl groups were explored as inhibitors of the PDZ2 domain of PSD-95. It was found that the ETAV sequence provided the best compromise between affinity, selectivity, size, and polarity, and although a range of potent (K_i = 1−2 μM) *N*-alkyl ETAV derivatives were identified, cyclohexylethyl-ETAV (**1**) with a K_i of 0.63 μM still proved to be the most potent compound.

To increase the stability of the peptides in human blood plasma, we developed synthetic approaches for selective introduction of thioamides into *N*-Me-ETAV (**31**). The peptides containing a thioamide bond between P^{-2} and P^{-3} (**45**) or between P^{-1} and P^{-2} (**41**) showed reduced affinity toward PDZ2, but introducing a thioamide between P^0 and P^{-1}, compound **35**, did not affect affinity. Because **35** showed complete stability in human blood plasma ($T_{1/2}$ > 5500 min), the three *N*-alkyl groups showing the best in vitro affinity for PDZ2, combined with a thioamide bond between P^{-1} and P^0 in the ETAV sequence, were prepared. This resulted in blood plasma-stable, N-alkylated thioamide containing tetrapeptides (**54**−**56**), which were equipotent to their corresponding N-alkylated tetrapeptides (**1**, **13**, and **14**).

Finally, **54**−**56** were found to be the most potent compounds in a cellular BRET assay, which reflects their ability to permeate cell membranes in COS-7 cells and disrupt the interaction between the C-terminal of the NMDA receptor and PDZ2. In conclusion, the thioamide derivatives **54**−**56** are potent and selective inhibitors of the PDZ2 domain of PSD-95, which show exceptional stability in blood plasma and disrupt the PSD-95/NMDA receptor interaction in living cells. Therefore, these compounds are excellent candidates for further studies of the biological importance of the PSD-95/NMDA receptor interaction, as well as leads for therapeutic development to establish the full potential of this interaction.

EXPERIMENTAL SECTION

Chemistry. Proton (^{1}H) NMR spectra were recorded on a Varian spectrometer, Mercury Plus (300 MHz) and carbon (^{13}C) NMR spectra were recorded on a Varian spectrometers, Gemini 2000 (75 MHz). Chemical shifts (δ) are reported in parts per million (ppm) with reference to tetramethylsilane (TMS) as an internal standard. The following abbreviations are used for the proton spectra multiplicities: s, singlet; br-s, broad singlet; d, doublet; dd, double doublet, triplet; q, quartet; and m, multiplet. Coupling constants (J) are reported in Hertz (Hz). Elemental analyses were performed by Mr. J. Theiner, Department of Physical Chemistry, University of Vienna, Austria. Preparative HPLC was performed on a Agilent 1200 system using a C18 reverse phase column (Zorbax 300 SB-C18, 21.2 mm × 250 mm) with a linear gradient of the binary solvent system of H_2O/ACN/TFA (A, 95/5/0.1, and B, 5/95/0.1) with a flow rate of 20 mL/min. Analytical HPLC was performed on an Agilent 1100 system with a C18 reverse phase column (Zorbax 300 SB-C18 column, 4.6 mm × 150 mm), flow rate of 1 mL/min, and a linear gradient of the binary solvent system of H_2O/ACN/TFA (A, 95/5/0.1, and B, 5/95/0.1). Mass spectra were obtained with an Agilent 6410 Triple Quadrupole Mass Spectrometer instrument using electron spray coupled to an Agilent 1200 HPLC system (ESI-LC/MS) with a C18 reverse phase column (Zorbax Eclipse XBD-C18, 4.6 mm × 50 mm), autosampler and diode array detector using a linear gradient of the binary solvent system of H_2O/ACN/formic acid (A, 95/5/0.1, and B, 5/95/0.086) with a flow rate of 1 mL/min. During ESI-LC/MS analysis, evaporative light scattering (ELS) traces were obtained with a Sedere Sedex 85 Light Scattering Detector. Compound identity of all tested compounds was confirmed by ESI-LC/MS, which also provided purity data (all >95%; UV and ELSD). High-resolution mass spectra (HRMS) were obtained using a Micromass Q-Tof 2 instrument and were all within ±5 ppm of theoretical values.

Peptide Synthesis. General Procedure. Peptides were manually synthesized by Fmoc-based SPPS using a MiniBlock (Mettler-Toledo, Columbus, OH). The 2-chlorotrityl chloride polystyrene resin (1−2% DVB cross-linking, 100−200 mesh) was used as a solid support, and after the resin swelled in dry DCM for 15−30 min, the first amino acid was loaded to the resin using diisopropylethylamine (DIPEA) (resin/amino acid/DIPEA in 1:4:8) in DCM for 1.5 h, followed by capping with methanol (DCM/MeOH/DIPEA 17:2:1). Fmoc deprotection was performed with 20% piperidine in DMF (1 × 5 and 1 × 15 min; wash step in between), and coupling of the consecutive amino acid was carried out with *O*-(benzotriazol-1-yl)-*N*,*N*,*N*′,*N*′-tetramethyluronium hexafluorophosphate (HBTU) and DIPEA (resin/amino acid/HBTU/DIPEA 1:4:4:4) in dry DMF (∼2 mL per 0.25 mmol resin) for 30 min. The final peptide was cleaved from the resin by treatment with TFA/TIPS/H_2O (90:5:5) for 2 h followed by evaporation in vacuo, cold ether precipitation, lyophilization, and HPLC purification. Compounds were lyophilized affording white or yellowish pure (>95%) solids. Fluorescent peptides (**57**−**61**) were synthesized by attaching 5-FAM (Anaspec, San Jose, CA) to the N-terminal of the respective resin-bound peptide by coupling with *O*-(7-azabenzotriazol-1-yl)-*N*,*N*,*N*′,*N*′-tetramethyluronium hexafluorophosphate (HATU) and 2,4,6-trimethylpyridine (Resin/5-FAM/HATU/2,4,6-trimethylpyridine 1:2:2:3) for 24 h in DMF, followed by cleavage from the resin and purification as described above.

***N*-Terminal Alkylation of Peptides. General Procedure (1, 8−30, and 63).** Tetrapeptides (0.25 mmol, 1 equiv) were synthesized on a 2-chlorotrityl chloride resin as described above followed by Fmoc deprotection, washing, and drying of the resin. The resin was swelled in DIPEA (6 equiv) in THF (2.5 mL) for ca. 30 min. 2-Nitrobenzenesulfonyl (Ns) chloride (4 equiv) in DCM (1 mL) was added slowly, while agitating the solution for 3 h followed by draining and washing with THF, MeOH, DCM, and THF (flow washes for 2 min). Subsequently, the resin was charged with nitrogen atmosphere, and the resin was treated with triphenylphosphine (2 M in THF, 5 equiv) and the alcohol (ROH, 10 equiv) in dry THF (1.0 mL) under nitrogen. Diisopropyl azadicarboxylate (DIAD) (1 M in THF, 5 equiv) was introduced slowly followed by agitation for 1 h at room temperature. The resin was drained and washed with THF and DCM (flow washes). Ns deprotection was carried out by swelling the resin in dry DMF (2 mL) followed by treatment with either (a) NaSPh (1 M, 2 mL) over a period of 3 × 1 h (intermediate flow washes in DMF) or (b) DBU (4 equiv) and mercaptoethanol (4 equiv) in 4 mL of dry DMF over a period of 4 × 0.5 h (intermediate flow washes in DMF). Finally, the resin was washed, and the product was cleaved from the resin, purified by HPLC, and characterized. Experimental details and characterization of **1**, **13**, **14**, and **31** have been described previously.[28]

*(S)-tert-Butyl 2-((S)-2-(((9H-Fluoren-9-yl)methoxy)carbonylamino)-propanamido)-3-methylbutanoate (**32**).* Triethylamine (3 mL) and HBTU (3.95 g, 10.4 mmol) were added to an ice-cooled slurry of Fmoc-Ala-OH (3.11 g, 10 mmol) and Val-O-*tert*-Bu·HCl (2.18 g, 10 mmol) in acetonitrile (40 mL). After it was stirred at room temperature for 2 h, the resulting white slurry was poured into brine (250 mL) and extracted with ethyl acetate (3 × 100 mL). The pooled extracts were successively washed with hydrochloric acid (2 M, 10 mL) and saturated sodium hydrogen carbonate (10 mL). After evaporation on Celite, the product was separated by automated flash chromatography on a stationary silica gel using ethyl acetate/heptane (1:4). Evaporation of the solvent and drying in a vacuum oven (10 Pa, 30 °C, 24 h) gave the protected dipeptide **32** (4.56 g, 98%) as a white crystalline mass; mp, 85−88 °C. ^{1}H NMR ($CDCl_3$): δ 0.85−0.91 (m, 6H), 1.39 (d, J = 6.9 Hz, 3H), 1.42 (s, 9H), 2.11−2.17 (m, 1H), 4.17 (t, J = 7.2 Hz, 1H), 4.33−4.35 (m, 2H), 4.41−4.46 (m, 2H), 5.83 (d, J = 7.7 Hz, 1H), 6.86 (d, J = 8.8 Hz, 1H), 7.22−7.27 (m, 2H), 7.31−7.36 (m, 2H), 7.55 (d, J = 6.9 Hz, 2H), 7.70 (d, J = 7.4 Hz, 2H). ^{13}C NMR ($CDCl_3$): δ 17.69, 19.03, 19.18, 28.06, 31.36, 47.05, 50.39, 57.58, 67.12, 81.84, 119.83, 125.06, 126.94, 127.55, 141.08, 143.72, 155.83, 170.61, 172.35. Anal. calcd for $C_{27}H_{34}N_2O_5$: C, 69.50; H, 7.35; N, 6.00. Found: C, 69.54; H, 7.45; N, 5.90.

*(R)-tert-Butyl 2-((S)-2-(((9H-Fluoren-9-yl)methoxy)carbonylamino)-propanethioamido)-3-methylbutanoate (**33**).* Compound **32** (0.23 g, 0.5 mmol) was dissolved in dry THF (10 mL), and Lawesson's reagent (0.24 g, 0.6 mmol) was added in one portion. Stirring was maintained at room temperature for 48 h under nitrogen. The resulting white slurry was poured into ice (100 mL) and extracted with ethyl acetate (3 × 30 mL). The pooled extracts were washed with water (10 mL), dried over magnesium sulfate, and evaporated on Celite. The product was separated by automated flash chromatography on a stationary silica gel column with ethyl acetate:heptane (1:4). Evaporation of the solvent and drying in a vacuum oven (10 Pa, 30 °C, 24 h) gave the thioamide **33** (0.20 g, 83%) as white crystals; mp, 134−135 °C. ^{1}H NMR ($CDCl_3$): δ 0.88 (d, J = 6.9 Hz, 3H), 0.93 (d, J = 6.6 Hz, 3H), 1.38 (s, 9H), 1.46 (d, J = 6.3 Hz, 3H), 2.21−2.23 (m, 1H), 4.17 (t, J = 7.3 Hz, 1H), 4.33−4.35 (m, 2H), 4.82−4.87 (m, 1H), 4.93−4.97 (m, 1H), 6.11 (d, J = 8.3 Hz, 1H), 7.21−7.27 (m, 2H), 7.30−7.35 (m, 2H), 7.56 (t, J = 7.7 Hz, 2H), 7.68 (d, J = 7.4 Hz, 2H), 8.82 (d, J = 7.7 Hz, 1H). ^{13}C NMR ($CDCl_3$): δ 18.54, 18.77, 22.55, 28.00, 31.01, 46.94, 55.79, 63.33, 67.34, 82.28, 119.81, 125.09, 126.92, 126.95, 127.56, 141.03, 143.54, 143.61, 155.61, 169.25, 205.60. Anal. calcd for $C_{27}H_{34}N_2O_4S$: C, 67.19; H, 7.10; N, 5.80; S, 6.64. Found: C, 66.96; H, 7.25; N, 5.71.

*(S)-2-((S)-2-(((9H-Fluoren-9-yl)methoxy)carbonylamino)propanethioamido)-3-methylbutanoic Acid (**34**).* Compound **33** (0.19 g, 0.4 mmol) was added in one portion to an ice-cooled mixture of TFA (10 mL) and DCM (4 mL), and stirring was maintained under nitrogen for 1 h. At this point, the reaction was complete according to TLC. Evaporation and drying in a vacuum oven (10 Pa, 35 °C, 12 h) quantitatively gave **34** as a thick colorless oil, which appeared pure on TLC and was used directly in the next step. ^{1}H NMR ($CDCl_3$): δ 0.94 (d, J = 6.7 Hz, 3H), 1.00 (d, J = 6.7 Hz, 3H), 1.44 (d, J = 6.1 Hz, 3H), 2.29−2.40 (m, 1H), 4.18 (t, J = 6.9 Hz, 1H), 4.28−4.39 (m, 2H), 4.72 (br-s, 1H), 5.08−5.16 (m, 1H), 5.88−5.91 (m, 1H), 7.23−7.29 (m, 2H), 7.34−7.39 (m, 2H), 7.54 (d, J = 6.9 Hz, 2H), 7.72 (d, J = 7.4 Hz, 2H), 8.63 (br-s, 1H). ^{13}C NMR ($CDCl_3$): δ 18.65, 18.70, 22.16, 30.97, 47.07, 56.19, 62.70, 67.65, 120.07, 125.12, 127.15, 127.83, 141.23, 143.56, 156.10, 174.83, 205.94. Anal. calcd for $C_{23}H_{26}N_2O_4S$: C, 64.77; H, 6.14; N, 6.57. Found: C, 64.89; H, 6.26; N, 6.43.

*N-Me-ETA$_5$V (**35**).* 2-Chlorotrityl chloride resin (0.16 g, loading 1.57 mmol/g) was shaken in dry DCM for 15 min and drained. Compound **34** (0.17 g, 0.4 mmol) dissolved in DCM (2 mL) containing DIPEA (0.35 mL) was added, and shaking was maintained for 2 h. After draining, the resin was washed three times with DCM/MeOH/DIPEA (17:2:1, 3 mL) and then flow washed with DCM and DMF. The resin was treated for 2 × 5 min with piperidine/DMF (3:7, 3 mL), drained, and washed twice with DMF. A solution of HBTU (0.38 g, 1 mmol), Fmoc-Thr(O-*tert*-Bu)-OH (0.40 g, 1 mmol), and DIPEA (0.17 mL) in DMF (1 mL) was added, and shaking was maintained for 30 min. After draining, the resin was washed twice with DMF and treated for 2 × 5 min with piperidine/DMF (3:7, 3 mL), drained, and washed twice with DMF. A solution of HBTU (0.38 g, 1 mmol), Fmoc-*N*-Me-Glu(O-*tert*-Bu)-OH (0.43 g, 1 mmol), and DIPEA (0.17 mL) in DMF (1 mL) was added, and shaking was maintained for 30 min. After draining, the resin was washed twice with DMF and then treated 2 × 5 min with piperidine/DMF (3:7, 3 mL), drained, and washed twice with DMF. An inhomogenous mixture of TFA/triisopropylsilane(TIPS)/H_2O (18:1:1, 5 mL) was added, and shaking was maintained for 2 h. The peptide containing solution was filtered into a flask and combined with two successive washes with DCM. After gentle evaporation in a stream of nitrogen, the crude peptide was washed with cold ether (2 × 10 mL) to give the crude product (0.16 g). Separation of 0.020 g by HPLC, evaporation, and lyophilization gave 11 mg (79%) of **35** as a white solid. ^{1}H NMR (CD_3OD): δ 1.01 (d, J = 6.6 Hz, 3H), 1.04 (d, J = 6.9 Hz, 3H), 1.22 (d, J = 6.3 Hz, 3H), 1.43 (d, J = 6.6 Hz, 3H), 2.18−2.31 (m, 3H), 2.53 (t, J = 7.4 Hz, 2H), 2.67 (s, 3H), 3.98 (t, J = 6.1 Hz, 1H), 4.21 (p, J = 4.4 Hz, 1H), 4.42 (d, J = 4.4 Hz, 1H), 4.84 (q, J = 6.9 Hz, 1H), 4.95 (d, J = 6.1 Hz, 1H). HRMS (ES^+) calcd for $C_{18}H_{33}N_4O_7S$ $[M + H]^+$, 449.2070; found, m/z 449.2064.

*(S)-tert-Butyl 2-((2S,3R)-2-(((9H-Fluoren-9-yl)methoxy)carbonylamino)-3-tert-butoxybutanamido)propanoate (**36**).* Triethylamine (3 mL) and HBTU (3.95 g, 10.4 mmol) were added to an ice-cooled slurry of Fmoc-Thr(O-*tert*-Bu)-OH (3.97 g, 10 mmol) and Ala-O-*tert*-Bu·HCl (1.89 g, 10 mmol) in acetonitrile (40 mL). After the solution was stirred at room temperature for 2 h, the resulting white slurry was poured into brine (250 mL) and extracted with ethyl acetate (3 × 100 mL). The pooled extracts were successively washed with hydrochloric acid (2 M, 10 mL) and saturated sodium hydrogen carbonate (10 mL). After evaporation on Celite, the product was separated by automated flash chromatography on a stationary silica gel using ethyl acetate/heptane (1:4). Evaporation of the solvent and drying in a vacuum oven (10 Pa, 30 °C, 24 h) gave the protected dipeptide **36** (4.56 g, 98%) as a white crystalline mass; mp, 70−72 °C. ^{1}H NMR ($CDCl_3$): δ 1.07 (d, J = 7.6 Hz, 3H), 1.10 (s, 9H), 1.26 (d, J = 7.2 Hz, 3H), 1.37 (s, 9H), 3.82−3.86 (m, 1H), 4.01−4.07 (m, 1H), 4.14−4.17 (m, 3H), 4.23−4.34 (m, 1H), 7.00 (d, J = 9.4 Hz, 1H), 7.29 (t, J = 7.3 Hz, 2H), 7.38 (t, J = 7.3 Hz, 2H), 7.70−7.74 (m, 2H), 7.85 (d, J = 7.4 Hz, 2H), 8.04 (d, J = 6.9 Hz, 1H). ^{13}C NMR ($CDCl_3$): δ 18.18, 20.32, 47.47, 49.03, 60.34, 66.52, 68.37, 74.36, 81.22, 120.73, 122.00, 125.95, 127.77, 128.25, 129.52, 141.35, 144.41, 156.45, 170.04, 172.03. Anal. calcd for $C_{30}H_{40}N_2O_6$: C, 68.68; H, 7.68; N, 5.34. Found: C, 68.35; H, 7.70; N, 5.18.

*(S)-tert-Butyl 2-((2S,3R)-2-(((9H-Fluoren-9-yl)methoxy)carbonylamino)-3-tert-butoxybutanethioamido)propanoate (**37**).* Compound **36** (2.65 g, 5 mmol) was dissolved in dry THF (100 mL), and Lawesson's reagent (2.43 g, 6 mmol) was added in one portion. Stirring was maintained at room temperature for 48 h under nitrogen. The resulting white slurry was poured into ice (400 mL) and extracted with ethyl acetate (3 × 100 mL). The pooled extracts were washed with water (25 mL), dried over magnesium sulfate, and evaporated on Celite. The product was separated by automated flash chromatography on a stationary silica gel column with ethyl acetate:heptane (1:4). Evaporation of the solvent and drying in a vacuum oven (10 Pa, 30 °C, 24 h) gave the thioamide **37** (1.75 g, 65%) as white crystals; mp, 132−133 °C. ^{1}H NMR ($CDCl_3$): δ 1.18 (d, J = 6.1 Hz, 3H), 1.33 (s, 9H), 1.51 (s, 9H), 1.53 (d, J = 11.8 Hz, 3H), 4.25−4.30 (m, 2H), 4.37−4.46 (m, 3H), 4.86 (t, J = 6.9 Hz, 1H), 6.63 (d, J = 5.2 Hz, 1H), 7.25−7.34 (m, 2H), 7.37−7.42 (m, 2H), 7.64 (t, J = 7.0 Hz, 2H), 7.75 (d, J = 7.4 Hz, 2H), 9.50 (d, J = 5.5 Hz, 1H). ^{13}C NMR ($CDCl_3$): δ 17.05, 17.18, 28.08, 28.37, 47.20, 54.74, 62.79, 67.15, 69.06, 75.63, 82.26, 119.88, 125.13, 125.21, 126.99, 127.61, 141.16, 143.56, 155.60, 170.54, 199.66. Anal. calcd for $C_{30}H_{40}N_2O_5S$: C, 66.64; H, 7.46; N, 5.18. Found: C, 66.62; H, 7.53; N, 5.07.

*Fmoc-TA$_5$V-O-tert-Bu (**39**).* Compound **37** (0.54 g, 1 mmol) was added in one portion to an ice-cold mixture of TFA (15 mL) and DCM (6 mL), and stirring was maintained under nitrogen for 1 h. After evaporation and drying in a vacuum oven (10 Pa, 35 °C, 12 h), the free acid **38** remained as a thick colorless oil. Val-O-*tert*-Bu·HCl (0.23 g, 1.1 mmol) and DMF (6 mL) were added, and the resulting slurry was stirred, while DIPEA (0.4 mL) and HATU (0.42 g, 1.1 mmol) were successively added during cooling in an ice bath, and stirring was maintained for 2 h at room temperature. The reaction mixture was poured into water and extracted with ethyl acetate (3 × 30 mL). The pooled organic phases were dried over sodium sulfate, filtered, and evaporated on Celite. The product was separated by automated flash chromatography on a stationary silica gel using ethyl acetate−heptane (1:1). Evaporation of the solvent and drying in a vacuum oven (10 Pa, 30 °C, 24 h) gave **39** (0.45 g, 77%) as a dark-yellow oil. ^{1}H NMR ($CDCl_3$): δ 0.82−0.93 (m, 6H), 1.01−1.27 (m, 6H), 1.41 (s, 9H), 1.99 (br-s, 1H), 2.04−2.18 (m, 1H), 3.98−4.17 (m, 3H), 4.19−4.58 (s, 3H), 4.98−5.07 (m, 1H), 6.26 (br-s, 1H), 6.84 (br-s, 1H), 7.17−7.37 (m, 4H), 7.50−7.72 (m, 4H), 9.11 (s, 1H). ^{13}C NMR ($CDCl_3$): δ 14.25, 14.31, 17.24, 17.72, 18.58, 28.08, 31.30, 47.01, 54.62, 57.85, 60.45, 63.80, 67.40, 68.89, 82.22, 119.84, 125.00, 126.94, 127.64, 141.13, 143.51, 156.39, 170.60, 171.14, 200.90. Anal. calcd for $C_{31}H_{41}N_3O_6S$: C, 63.78; H, 7.08; N, 7.20. Found: C, 64.12; H, 7.43; N, 6.90.

*Fmoc-E(O-tert-Bu)T$_5$AV-O-tert-Bu (**40**).* Compound **39** (0.29 g, 0.5 mmol) was dissolved in a dimethylamine solution (2.0 M in MeOH, 4 mL, 8 mmol), and stirring was maintained for 2 h. After evaporation in a stream of air, THF (4 mL) was added and successively evaporated in a stream of air in order to remove traces of dimethylamine. The residue was placed in a vacuum oven (10 Pa, 30 °C, 24 h), dissolved in DMF (3 mL), and cooled in an ice bath, while Fmoc-*N*-Me-Glu(O-*tert*-Bu)-OH (0.21 g, 0.55 mmol), DIPEA (0.2 mL), and HATU (0.21 g, 0.55 mmol) were successively added. After it was stirred at room temperature for 2 h, the reaction mixture was poured into water (40 mL) and extracted with ethyl acetate (3 × 30 mL). The pooled organic phases were dried over sodium sulfate, filtered, and evaporated on Celite. The product was separated by automated flash chromatography on a stationary silica gel using ethyl acetate−heptane (1:1). Evaporation of the solvent and drying in a vacuum oven (10 Pa, 30 °C, 24 h) gave **40** (0.13 g, 33%) as a thick colorless oil. ^{1}H NMR (DMSO-d_6): δ 0.85 (d, J = 3.3 Hz, 3H), 0.87 (d, J = 3.0 Hz, 3H), 1.03 (d, J = 5.8 Hz, 3H), 1.36 (s, 18H), 1.79 (br-s, 1H), 1.96−2.07 (m, 3H), 2.66 (s, 3H), 2.68−2.76 (m, 3H), 4.02 (t, J = 6.6 Hz, 2H), 4.27−4.40 (m, 4H), 4.50−4.65

(m, 2H), 4.89−4.99 (m, 2H), 7.27−7.40 (m, 4H), 7.60 (d, J = 7.2 Hz, 2H), 7.72 (d, J = 6.9 Hz, 1H), 7.84 (d, J = 7.4 Hz, 2H), 8.07 (d, J = 7.7 Hz, 1H), 9.73 (d, J = 6.1 Hz, 1H). ^{13}C NMR (DMSO-d_6): δ 18.24, 18.80, 19.74, 20.82, 24.30, 28.41, 28.53, 30.57, 32.23, 39.00, 47.48, 54.33, 58.32, 58.80, 65.10, 67.66, 68.92, 80.36, 81.19, 120.72, 125.72, 127.74, 128.27, 141.34, 144.33, 156.71, 170.26, 170.73, 171.49, 172.04, 201.03. Anal. calcd for $C_{41}H_{58}N_4O_9S$: C, 62.89; H, 7.47; N, 7.16. Found: C, 62.54; H, 7.25; N, 7.40.

N-Me-ET$_5$AV (***41***). A dimethylamine solution (2.0 M in MeOH, 2 mL, 4 mmol) was added to **40** (0.04 g, 0.05 mmol). After it was stirred for 1 h, the reaction mixture was evaporated to dryness in a stream of nitrogen. TFA (2 mL) was added, and stirring was maintained at room temperature for 2 h. After evaporation, the product was separated by HPLC. Evaporation of solvent and lyophilization gave **41** (16 mg, 71%) as a thick colorless oil. ^{1}H NMR (CD_3OD): δ 0.98 (d, J = 6.6 Hz, 6H), 1.22 (d, J = 6.3 Hz, 3H), 1.49 (d, J = 7.2 Hz, 3H), 2.14−2.19 (m, 3H), 2.51 (t, J = 7.4 Hz, 2H), 2.68 (s, 3H), 3.97 (t, J = 6.0 Hz, 1H), 4.08 (p, J = 6.1 Hz, 1H), 4.30 (q, J = 5.2 Hz, 1H), 4.66 (d, J = 6.1 Hz, 1H), 4.96 (d, J = 7.2 Hz, 1H). HRMS (ES$^+$) calcd for $C_{18}H_{33}N_4O_7S$ $[M + H]^+$, 449.2070; found, m/z 449.2060.

Fmoc-N-Me-E(O-tert-Bu)T(O-tert-Bu)-O-TBDPS (***43***). 2-Chlorotrityl chloride resin (0.33 g, loading 1.57 mmol/g) was shaken in dry DCM for 15 min and then drained. Fmoc-Thr(O-*tert*-Bu)-OH (0.60 g, 1.5 mmol) dissolved in DCM (5 mL) containing DIPEA (1 mL) was added, and shaking was maintained for 2 h. After draining, the resin was washed three times with DCM/MeOH/DIPEA (17:2:1, 5 mL) and then flow washed with DCM and DMF. The resin was treated 2 × 5 min with piperidine/DMF (3:7, 5 mL), drained, and washed twice with DMF. A solution of HBTU (0.38 g, 1 mmol), Fmoc-*N*-Me-Glu(O-*tert*-Bu)-OH (0.44 g, 1 mmol), and DIPEA (0.4 mL) in DMF (2 mL) was added, and shaking was maintained for 30 min. After draining, the resin was washed three times with DMF (10 mL) and then three times with DCM (10 mL). A mixture of HFIP and DCM (1:4, 15 mL) was added, and shaking was maintained for 5 min. The peptide-containing solution was filtered into a flask and combined with two successive washes with DCM. After gentle evaporation in a stream of nitrogen, the residue (**42**) was dissolved in DMF (5 mL) containing DIPEA (1 mL), and TBDPS chloride (0.52 mL, 2 mmol) was added. The reaction was stirred at room temperature for 2 h, poured into water (55 mL) containing brine (5 mL), and extracted with ethyl acetate (3 × 30 mL). The pooled extracts were successively washed with hydrochloric acid (2 M, 10 mL) and saturated sodium hydrogen carbonate (10 mL). After evaporation on Celite, the product was separated by automated flash chromatography on a stationary silica gel using ethyl acetate/heptane (1:9). Evaporation of the solvent and drying in a vacuum oven (10 Pa, 30 °C, 24 h) gave the protected dipeptide **43** (0.30 g, 72%) as a colorless oil. ^{1}H NMR ($CDCl_3$): δ 0.95 (s, 9H), 1.12 (s, 9H), 1.26 (d, J = 7.0 Hz, 3H), 1.43 (s, 9H), 2.12−2.26 (m, 4H), 2.87 (s, 3H), 4.20−4.27 (m, 3H), 4.42 (d, J = 6.6 Hz, 2H), 4.54 (d, J = 8.5 Hz, 1H), 6.77 (d, J = 8.0 Hz, 1H), 7.20−7.39 (m, 9H), 7.55−7.57 (m, 2H), 7.64−7.55 (m, 7H). ^{13}C NMR ($CDCl_3$): δ 19.56, 21.36, 23.62, 27.28, 28.47, 28.77, 30.64, 32.41, 58.60, 59.34, 67.28, 68.32, 74.29, 80.77, 120.20, 125.21, 127.29, 127.86, 127.92, 130.37, 131.30, 131.43, 135.86, 141.46, 144.01, 157.26, 169.94, 170.44, 172.07. Anal. calcd for $C_{49}H_{62}N_2O_8Si$: C, 70.47; H, 7.48; N, 3.35. Found: C, 70.13; H, 7.18; N, 3.02.

Fmoc-N-Me-E(O-tert-Bu)$_5$T(O-tert-Bu)-O-TBDPS (***44***). Compound **43** (0.17 g, 0.2 mmol) was dissolved in dry THF (3 mL), and Lawesson's reagent (0.10 g, 0.25 mmol) was added in one portion. Stirring was maintained at room temperature for 48 h under nitrogen. The resulting white slurry was poured into water (15 mL) and extracted with ethyl acetate (3 × 20 mL). The pooled extracts were dried over magnesium sulfate and evaporated on Celite. The product was separated by automated flash chromatography on a stationary silica gel column with ethyl acetate:heptane (1:9). Evaporation of the solvent and drying in a vacuum oven (10 Pa, 30 °C, 24 h) gave the thioamide **44** (0.12 g, 70%) as a colorless oil. ^{1}H NMR ($CDCl_3$): δ 0.93 (s, 9H), 1.06 (s, 9H), 1.16 (d, J = 6.8 Hz, 3H), 1.43 (s, 9H), 2.15−2.24 (m, 4H), 2.92 (s, 3H), 4.10−4.39 (m, 4H), 4.90−4.98 (m, 1H), 5.18 (d, J = 8.3 Hz, 1H), 7.22−7.46 (m, 9H), 7.52−7.56 (m, 2H), 7.67−7.85 (m, 7H), 7.78 (br-s, 1H). ^{13}C NMR ($CDCl_3$): δ 19.36, 26.83, 27.13, 28.31, 28.56, 30.15, 32.41, 43.32, 55.58, 63.49, 64.46, 66.86, 68.28, 74.44, 80.64, 120.02, 125.09, 127.15, 127.68, 130.43, 131.17, 134.80, 135.76, 141.26, 143.37, 157.11, 165.17, 171.89, 202.40. Anal. calcd for $C_{49}H_{62}N_2O_7SSi$: C, 68.14; H, 7.34; N, 3.29. Found: C, 68.51; H, 7.53; N, 3.48.

N-Me-E$_5$TAV (***45***). 2-Chlorotrityl chloride resin (0.33 g, loading 1.57 mmol/g) was shaken in dry DCM for 15 min and drained. Fmoc-Val-OH (0.34 g, 1 mmol) dissolved in DCM (3 mL) containing DIPEA (0.5 mL) was added, and shaking was maintained for 2 h. After draining, the resin was washed three times with DCM/MeOH/DIPEA (17:2:1, 3 mL) and then flow washed with DCM and DMF. The resin was treated 2 × 5 min with piperidine/DMF (3:7, 3 mL), drained, and washed twice with DMF. A solution of HATU (0.38 g, 1 mmol), Fmoc-Ala-OH (0.31 g, 1 mmol), and DIPEA (0.17 mL) in DMF (1 mL) was added, and shaking was maintained for 30 min. After draining, the resin was washed twice with DMF and then treated 2 × 5 min with piperidine/DMF (3:7, 3 mL), drained, and washed twice with DMF. Compound **44** (0.12 g, 0.14 mmol) was treated with a TBAF solution (1.0 M in THF, 1 mL, 1 mmol) for 1 h under nitrogen. The reaction mixture was evaporated to dryness in a stream of nitrogen, and the residue was redissolved in a solution of DIPEA (0.2 mL) and HATU (0.065 g, 0.17 mmol) in DMF (1 mL) and added to the resin. After it was shaken for 30 min, the resin was drained, washed twice with DMF treated 2 × 5 min with piperidine/DMF (3:7, 3 mL), drained, and washed twice with DMF. An inhomogenous mixture of TFA/TIPS/H_2O (18:1:1, 3 mL) was added, and shaking was maintained for 2 h. The peptide containing solution was filtered into a flask and combined with two successive washes with DCM. After gentle evaporation in a stream of nitrogen, the crude peptide was washed with cold ether (2 × 5 mL). Separation of the product by HPLC, evaporation and lyophilization gave 11 mg (18%) of **45** as a white solid. ^{1}H NMR (CD_3OD): δ 1.00 (d, J = 6.5 Hz, 6H), 1.23 (d, J = 6.2 Hz, 3H), 1.47 (d, J = 6.7 Hz, 3H), 2.13−2.25 (m, 3H), 2.52 (t, J = 7.4 Hz, 2H), 2.70 (s, 3H), 3.99 (t, J = 5.8 Hz, 1H), 4.11−4.18 (m, 2H), 4.69 (d, J = 5.7 Hz, 1H), 5.08 (d, J = 7.2 Hz, 1H). HRMS (ES$^+$) calcd for $C_{18}H_{33}N_4O_7S$ $[M + H]^+$, 449.2070; found, m/z 449.2082.

General Procedure for Synthesis of Thioamide Containing *N*-Alkylated Tetrapeptides (54−56). Fmoc-A$_S$V-O-*tert*-Bu (**33**) was treated with DCM/TFA (0.4:1) at room temperature for 1 h and concentrated to a colorless foam. The foam was redissolved in dry THF and concentrated three times to remove residual TFA. After it was dried in vacuo for 3 h, the product was dissolved in dry DCM, and DIPEA (10 equiv) was added, treating a preswelled 2-chlorotrityl chloride resin with this mixture. After it was agitated for 12 h, followed by capping of unreacted sites with DCM/MeOH/DIPEA (17:2:1) (3 × 1 min) and flow washes with DCM, the loaded resin was dried in vacuo. Fmoc deprotection and HBTU coupling of Fmoc-Thr(O-*tert*-Bu)-OH was achieved as described under general peptide synthesis to get resin **53**. Resin loading of the tripeptide (**53**) was determined to be 0.44 mmol/g resin corresponding to a 0.11 mmol scale. Fmoc-Glu(O-*tert*-Bu)-OH (0.25 mmol scale) was loaded, Fmoc deprotected, Ns protected, and N-terminally alkylated with the desired alcohol as described under general N-alkylation procedure and cleaved from the resin using 20% HFIP in DCM for 5 min. After the resin was washed with DCM, the filtrate was concentrated and dried in high vacuo affording the N-alkylated glutamates (**50**−**52**) as oils. The N-alkylated amino acids (1.1−2.0 equiv), **50**, **51**, or **52**, were dissolved in dry DMF (2.5 mL), and HATU (1.5−2.0 equiv) and HOAt (1.5−2.0 equiv) were added. This mixture was added to the preswelled resin (**53**) (0.11 mmol scale) before adding collidine (3.0−4.0 equiv) during agitation. After coupling for 1 h, the resin was drained and washed with DCM and DMF. Ns deprotection

(DBU/mercaptoethanol), cleavage, and purification of the final peptides were conducted as described under general peptides synthesis.

*N-Cyclohexylethyl-ETA$_5$V (**54**).* White solid; yield, 12 mg (20%). ^{1}H NMR (CD_3OD) δ (ppm): 0.89−1.08 (m, 2H), 1.03 (dd, J = 7.2, 10.4 Hz, 6H), 1.15−1.41 (m, 4H) 1.23 (d, J = 6.9 Hz, 3H), 1.43 (d, J = 6.9 Hz, 3H), 1.59 (q, J = 8.0 Hz, 2H), 1.64−1.80 (m, 5H), 2.12−2.22 (m, 2H) 2.22−2.35 (m, 1H) 2.55 (t, J = 7.2 Hz, 2H), 2.91−3.04 (m, 2H), 3.95−4.02 (m, 1H), 4.17−4.27 (m, 1H), 4.40−4.44 (m, 1H), 4.93−4.97 (m, 1H). MS (ES$^+$): m/z 545.29. HRMS (ES$^+$) calcd for $C_{25}H_{45}N_4O_7S$ [M + H]$^+$, 545.3009; found, m/z 545.3027.

*N-(Naphthalene-2-yl)ethyl-ETA$_5$V (**55**).* White solid; yield, 7 mg (11%). ^{1}H NMR (CD_3OD) δ (ppm): 1.03 (dd, J = 6.7, 10.7 Hz, 6H), 1.20 (d, J = 6.3 Hz, 3H), 1.43 (d, J = 6.9 Hz, 3H), 2.17−2.37 (m, 3H), 2.57 (t, J = 6.9 Hz, 2H), 3.13−3.23 (m, 2H), 4.00−4.08 (m, 1H), 4.15−4.25 (m, 1H), 4.41−4.44 (m, 1H), 7.38 (dd, J = 1.8, 8.2 Hz, 1H) 7.42−7.51 (m, 2H), 7.73−7.75 (m, 1H), 7.78−7.87 (m, 3H). MS (ES$^+$): m/z 589.30. HRMS (ES$^+$) calcd for $C_{29}H_{41}N_4O_7S$ [M + H]$^+$, 589.2696; found, m/z 589.2708.

*N-(3,4-Dichlorophenyl)ethyl-ETA$_5$V (**56**).* White solid; yield, 12 mg (18%). ^{1}H NMR (CD_3OD) δ (ppm): 1.03 (dd, J = 7.0, 10.2 Hz, 6H), 1.21 (d, J = 6.3 Hz, 3H), 1.43 (d, J = 6.5 Hz, 3H), 2.16−2.34 (m, 3H), 2.56 (t, J = 7.4 Hz, 2H), 2.99 (t, J = 8.4, 2H), 3.13−3.27 (m, 2H), 3.98−4.07 (m, 1H), 4.14−4.24 (m, 1H), 4.41 (d, J = 4.9 Hz, 1H), 4.96 (d, J = 6.2 Hz, 1H), 7.20 (dd, J = 2.5, 8.1 Hz, 1H) 7.44−7.51 (m, 2H). MS (ES$^+$): m/z 607.20. HRMS (ES$^+$) calcd for $C_{25}H_{37}Cl_2N_4O_7S$ [M + H]$^+$, 607.1760; found, m/z 607.1757.

Molecular Modeling[28]. PDZ1 and PDZ2 were aligned with PDZ3 using Prime (Version 1.6, Schrödinger, LLC, New York, NY). From these sequences, homology models were created using the PDZ3 X-ray crystal structure (PDB structure 1BE9)[37] as a template in Prime with standard parameters. The peptide ligand from 1BE9, KQTSV, was rebuilt to IESDV in the homology models. The side chains of the PDZ domain and the peptide were then minimized in Macromodel (Version 9.5, Schrödinger, LLC, New York, NY) using the force field OPLS2005 and by constraining the backbone. A grid around the peptide was generated in Glide (Version 4.5, Schrödinger, LLC, New York, NY) and used for docking. Relevant peptides were docked flexibly in Glide using default parameters including postdocking minimization. The conserved water molecule seen in the binding pocket was kept constant during docking and minimization. Pymol, version 0.97, was used for creating figures.[52]

FP Assay. FP measurements were performed as previously described.[28] In short, PDZ saturation binding assays were conducted to determine K_d values for fluorescent-labeled peptides Cy5-GluN2B and Cy5-CRIPT toward PDZ2 and PDZ3 domains of PSD-95, respectively, in vitro. To measure the affinities (IC_{50} values) for nonfluorescent compounds and PDZ domains, heterologous competition binding assays were performed by adding increasing concentrations of compounds to a fixed concentration of labeled peptide (50 nM) and PDZ domain (3 μM for PDZ2 and 5 μM for PDZ3). FP values were fitted to the general equation (eq 1):

$$Y = \text{bottom} + (\text{top} - \text{bottom})/[1 + (10^{(X - \log IC_{50})*\text{Hill slope}})] \quad (1)$$

where X is the logarithmic value of peptide concentration and Y is the experimental FP values. IC_{50} values were used to calculate the competitive inhibition constant, K_i.[53] All values reported are the average of at least three individual experiments.

Human Blood Plasma Stability Assay[35]. Compounds were dissolved in human blood plasma (270 μL, normal human plasma, pooled, 3H Biomedical, Uppsala, Sweden) to a concentration of 0.25 mM (30 μL of 2.5 mM) and incubated at 37 °C. Aliquots (30 μL) were removed at various time intervals and quenched with 5% aqueous trichloroacetic acid (60 μL). The aliquots were vortexed and incubated for 15 min at 4 °C prior to centrifugation at 18000g for 2 min. The supernatants were analyzed by ESI-LC/MS using the ELS or UV_{214} signals for quantification relative to time zero, and the total ion current (TIC) trace was used to identify the compounds (m/z). Procaine (positive control) and procainamide (negative control) were investigated at 50 μM. Ligand recovery after the precipitation procedure was between 85 and 95%.

Cell Permeability. COS-7 cells growing on 13 nm plastic coverslips (Nalge Nunc International, Rochester, NY) in 12-well plates at 80−90% confluence were washed with PBS and incubated with DMEM with 10% (v/v) FBS (200 μL) containing fluorophore-labeled peptides (10 μM) at 37 °C for 1 h. Cells were then washed five times with ice-cold PBS and fixed by incubation in 4% (v/v) paraformaldehyde in PBS for 10 min at room temperature followed by 10 min on ice. Coverslips were subsequently mounted on microscope slides (Sigma-Aldrich PolyprepTM slides, Steinheim, Germany) using SlowFade Antifade kit (Invitrogen) and sealed with nail polish. Confocal imaging was performed on a Zeiss LSM 510 confocal laser scanning microscope (Carl Zeiss, Jena, GmBH, Germany), using a Zeiss plan apochromat 63× oil immersion objective. Fluorophores were excited using an argon laser line at 458 nm. The confocal images were overlaid transmitted light images to verify the localization of cells.

BRET Assay. COS-7 cells were transfected with the mammalian expression plasmids pGFP^2-PDZ2 and pRluc-N2B vectors in a 1:1 ratio and seeded into white 96-well plates as described previously.[49] At 24−28 h post-transfection, cells were washed twice with PBSCM (100 μL, 137 mM NaCl, 2.7 mM KCl, 10 mM Na_2HPO_4, 1.76 mM KH_2PO_4, 0.5 mM $MgCl_2$, and 0.1 mM $CaCl_2$, pH 7.4) per well and incubated at room temperature for 40 min with test compounds dissolved in PBSCM (50 μL). DeepBlueC coelenterazine from a freshly prepared solution in PBSCM was added to each well to a final concentration of 5 μM. Five seconds after the addition of DeepBlueC coelenterazine, measurements of luminescence and fluorescence from each well were performed using a Mithras LB 940 plate reader (Berthold Technologies GmbH & Co., Germany) by counting the long- and shortwave emission using 410 (80 nm bandwidth) and 515 nm (40 nm bandwidth) emission filters, respectively. Background emission of luminescence and fluorescence was determined from wells containing mock-transfected cells. For each well, the BRET signal was calculated as:

$$\frac{E_{515} - \text{background}_{515}}{E_{410} - \text{background}_{410}}$$

where E_{515} is the fluorescence emission, E_{410} is the luminescence emission, background_{515} is the background fluorescence, and background_{410} is the background luminescence. The obtained BRET signal was corrected for BRET produced by cross-talk of the strong luminescence signal into the fluorescence signal by subtracting the BRET signal obtained in parallel from COS-7 cells expressing only the donor protein (i.e., cells cotransfected with Rluc-fusion protein plasmid and empty pcDNA3.1). GraphPad Prism version 4.03 was used for statistical analysis (Student's t test, one- and two-way ANOVA).

■ ASSOCIATED CONTENT

Supporting Information. Experimental procedures and data for compound **19**−**30** and their corresponding alcohol intermediates. This material is available free of charge via the Internet at http://pubs.acs.org.

■ AUTHOR INFORMATION

Corresponding Author

*Tel: +45 3533 6114. Fax: +45 3533 6041. E-mail: krst@farma.ku.dk.

Author Contributions

†These authors contributed equally to this work.

■ ACKNOWLEDGMENT

This work was supported by the Lundbeck Foundation (K.S.), The Danish Council for Independent Research | Medical Sciences (K.S.) and the Danish Council for Independent Research | Technology and Production Sciences (A.B). We thank Martin Røder for initial assistance in the synthesis of thioamide peptides and Signe Egstrand Andersen and Mie Vindahl Andersen for the preparation of selected peptides.

■ ABBREVIATIONS USED

BRET, bioluminescence resonance energy transfer; FP, fluorescence polarization; nNOS, neuronal nitric oxide synthase; NO, nitric oxide; NMDA, *N*-methyl-D-aspartate; PDZ, PSD-95, discs large, zonula occludens-1; PPIs, protein−protein interactions; PSD-95, postsynaptic density-95; SAR, structure−activity relationship

■ REFERENCES

(1) Arkin, M. R.; Wells, J. A. Small-molecule inhibitors of protein-protein interactions: Progressing towards the dream. *Nat. Rev. Drug Discovery* **2004**, *3*, 301–317.

(2) Wells, J. A.; Mcclendon, C. L. Reaching for high-hanging fruit in drug discovery at protein-protein interfaces. *Nature* **2007**, *450*, 1001–1009.

(3) Dev, K. K. Making protein interactions druggable: Targeting PDZ domains. *Nat. Rev. Drug Discovery* **2004**, *3*, 1047–1056.

(4) Gardoni, F.; Di Luca, M. New targets for pharmacological intervention in the glutamatergic synapse. *Eur. J. Pharmacol.* **2006**, *545*, 2–10.

(5) Wen, W.; Wang, W.; Zhang, M. Targeting PDZ domain proteins for treating NMDA receptor-mediated excitotoxicity. *Curr. Top. Med. Chem.* **2006**, *6*, 711–721.

(6) Wang, N. X.; Lee, H. J.; Zheng, J. J. Therapeutic use of PDZ protein-protein interaction antagonism. *Drug News Perspect.* **2008**, *21*, 137–141.

(7) Blazer, L. L.; Neubig, R. R. Small molecule protein-protein interaction inhibitors as CNS therapeutic agents: Current progress and future hurdles. *Neuropsychopharmacology* **2009**, *34*, 126–141.

(8) Kim, E.; Niethammer, M.; Rothschild, A.; Jan, Y. N.; Sheng, M. Clustering of shaker-type K^+ channels by interaction with a family of membrane-associated guanylate kinases. *Nature* **1995**, *378*, 85–88.

(9) Kim, E.; Sheng, M. PDZ domain proteins of synapses. *Nat. Rev. Neurosci.* **2004**, *5*, 771–781.

(10) Elias, G. M.; Nicoll, R. A. Synaptic trafficking of glutamate receptors by MAGUK scaffolding proteins. *Trends Cell Biol.* **2007**, *17*, 343–352.

(11) Sheng, M.; Sala, C. PDZ domains and the organization of supramolecular complexes. *Annu. Rev. Neurosci.* **2001**, *24*, 1–29.

(12) Traynelis, S. F.; Wollmuth, L. P.; Mcbain, C. J.; Menniti, F. S.; Vance, K. M.; Ogden, K. K.; Hansen, K. B.; Yuan, H.; Myers, S. J.; Dingledine, R.; Sibley, D. Glutamate receptor ion channels: Structure, regulation, and function. *Pharmacol. Rev.* **2010**, *62*, 405–496.

(13) Dawson, V. L.; Dawson, T. M.; London, E. D.; Bredt, D. S.; Snyder, S. H. Nitric oxide mediates glutamate neurotoxicity in primary cortical cultures. *Proc. Natl. Acad. Sci. U.S.A.* **1991**, *88*, 6368–6371.

(14) Sattler, R.; Xiong, Z.; Lu, W. Y.; Hafner, M.; Macdonald, J. F.; Tymianski, M. Specific coupling of NMDA receptor activation to nitric oxide neurotoxicity by PSD-95. *Protein Sci.* **1999**, *284*, 1845–1848.

(15) Garber, K. Stroke treatment-light at the end of the tunnel? *Nat. Biotechnol.* **2007**, *25*, 838–840.

(16) Ikonomidou, C.; Turski, L. Why did NMDA receptor antagonists fail clinical trials for stroke and traumatic brain injury?. *Lancet Neurol.* **2002**, *1*, 383–386.

(17) Christopherson, K. S.; Hillier, B. J.; Lim, W. A.; Bredt, D. S. PSD-95 assembles a ternary complex with the *N*-methyl-D-aspartic acid receptor and a bivalent neuronal NO synthase PDZ domain. *J. Biol. Chem.* **1999**, *274*, 27467–27473.

(18) Aarts, M.; Liu, Y.; Liu, L.; Besshoh, S.; Arundine, M.; Gurd, J. W.; Wang, Y. T.; Salter, M. W.; Tymianski, M. Treatment of ischemic brain damage by perturbing NMDA receptor-PSD-95 protein interactions. *Science* **2002**, *298*, 846–850.

(19) Soriano, F. X.; Martel, M. A.; Papadia, S.; Vaslin, A.; Baxter, P.; Rickman, C.; Forder, J.; Tymianski, M.; Duncan, R.; Aarts, M.; Clarke, P.; Wyllie, D. J.; Hardingham, G. E. Specific targeting of pro-death NMDA receptor signals with differing reliance on the NR2B PDZ ligand. *J. Neurosci.* **2008**, *28*, 10696–10710.

(20) LeBlanc, B. W.; Iwata, M.; Mallon, A. P.; Rupasinghe, C. N.; Goebel, D. J.; Marshall, J.; Spaller, M. R.; Saab, C. Y. A cyclic peptide targeted against PSD-95 blocks central sensitization and attenuates thermal hyperalgesia. *Neuroscience* **2010**, *167*, 490–500.

(21) Florio, S. K.; Loh, C.; Huang, S. M.; Iwamaye, A. E.; Kitto, K. F.; Fowler, K. W.; Treiberg, J. A.; Hayflick, J. S.; Walker, J. M.; Fairbanks, C. A.; Lai, Y. Disruption of nNOS-PSD95 protein-protein interaction inhibits acute thermal hyperalgesia and chronic mechanical allodynia in rodents. *Br. J. Pharmacol.* **2009**, *158*, 494–506.

(22) Tao, F.; Su, Q.; Johns, R. A. Cell-permeable peptide Tat-PSD-95 PDZ2 inhibits chronic inflammatory pain behaviors in mice. *Mol. Ther.* **2008**, *16*, 1776–1782.

(23) Ittner, L. M.; Ke, Y. D.; Delerue, F.; Bi, M.; Gladbach, A.; Van Eersel, J.; Wolfing, H.; Chieng, B. C.; Christie, M. J.; Napier, I. A.; Eckert, A.; Staufenbiel, M.; Hardeman, E.; Götz, J. Dendritic function of tau mediates amyloid-β toxicity in Alzheimer's disease mouse models. *Cell* **2010**, *142*, 387–397.

(24) Lim, I. A.; Hall, D. D.; Hell, J. W. Selectivity and promiscuity of the first and second PDZ domains of PSD-95 and synapse-associated protein 102. *J. Biol. Chem.* **2002**, *277*, 21697–21711.

(25) Hung, A. Y.; Sheng, M. PDZ domains: Structural modules for protein complex assembly. *J. Biol. Chem.* **2002**, *277*, 5699–5702.

(26) Songyang, Z.; Fanning, A. S.; Fu, C.; Xu, J.; Marfatia, S. M.; Chishti, A. H.; Crompton, A.; Chan, A. C.; Anderson, J. M.; Cantley, L. C. Recognition of unique carboxyl-terminal motifs by distinct PDZ domains. *Science* **1997**, *275*, 73–77.

(27) Stiffler, M. A.; Chen, J. R.; Grantcharova, V. P.; Lei, Y.; Fuchs, D.; Allen, J. E.; Zaslavskaia, L. A.; Macbeath, G. PDZ domain binding selectivity is optimized across the mouse proteome. *Science* **2007**, *317*, 364–369.

(28) Bach, A.; Chi, C. N.; Olsen, T. B.; Pedersen, S. W.; Røder, M. U.; Pang, G. F.; Clausen, R. P.; Jemth, P.; Strømgaard, K. Modified peptides as potent inhibitors of the postsynaptic density-95/*N*-methyl-D-aspartate receptor interaction. *J. Med. Chem.* **2008**, *51*, 6450–6459.

(29) Bach, A.; Stuhr-Hansen, N.; Thorsen, T. S.; Bork, N.; Moreira, I. S.; Frydenvang, K.; Padrah, S.; Christensen, S. B.; Madsen, K. L.; Weinstein, H.; Gether, U.; Strømgaard, K. Structure-activity relationships of a small-molecule inhibitor of the PDZ domain of PICK1. *Org. Biomol. Chem.* **2010**, *8*, 4281–4288.

(30) Hajduk, P. J.; Huth, J. R.; Fesik, S. W. Druggability indices for protein targets derived from NMR-based screening data. *J. Med. Chem.* **2005**, *48*, 2518–2525.

(31) Fry, D. C.; Vassilev, L. T. Targeting protein-protein interactions for cancer therapy. *J. Mol. Med.* **2005**, *83*, 955–963.

(32) Piserchio, A.; Salinas, G. D.; Li, T.; Marshall, J.; Spaller, M. R.; Mierke, D. F. Targeting specific PDZ domains of PSD-95; Structural basis for enhanced affinity and enzymatic stability of a cyclic peptide. *Chem. Biol.* **2004**, *11*, 469–473.

(33) Hammond, M. C.; Harris, B. Z.; Lim, W. A.; Bartlett, P. A. β Strand peptidomimetics as potent PDZ domain ligands. *Chem. Biol.* **2006**, *13*, 1247–1251.

(34) Udugamasooriya, D. G.; Sharma, S. C.; Spaller, M. R. A chemical library approach to organic-modified peptide ligands for PDZ domain proteins: A synthetic, thermodynamic and structural investigation. *ChemBioChem* **2008**, *9*, 1587–1589.

(35) Bach, A.; Chi, C. N.; Pang, G. F.; Olsen, L.; Kristensen, A. S.; Jemth, P.; Strømgaard, K. Design and synthesis of highly potent and

plasma-stable dimeric inhibitors of the PSD-95/NMDA receptor interaction. *Angew. Chem., Int. Ed.* **2009**, *48*, 9685–9689.

(36) www.clinicaltrials.gov.

(37) Doyle, D. A.; Lee, A.; Lewis, J.; Kim, E.; Sheng, M.; Mackinnon, R. Crystal structures of a complexed and peptide-free membrane protein-binding domain: Molecular basis of peptide recognition by PDZ. *Cell* **1996**, *85*, 1067–1076.

(38) Spatola, A. F. Peptide backbone modifications: Structure-activity analysis of peptides containing amide bond surrogates. In *Chemistry and Biochemistry of Amino Acids, Peptides and Proteins*; Weinstein, B., Ed.; Marcel Dekker: New York, 1983; Vol. 7, pp 267−357.

(39) Mock, W. L.; Chen, J.-T.; Tsang, J. W. Hydrolysis of a thiopeptide by cadmium carboxypeptidase A. *Biochem. Biophys. Res. Commun.* **1981**, *102*, 389–396.

(40) Campbell, P.; Nashed, N. T. Carboxypeptidase A catalyzed hydrolysis of thiopeptide and thioester analogs of specific substrates. An effect on k_{cat} for peptide, but not ester, substrates. *J. Am. Chem. Soc.* **1982**, *104*, 5221–5226.

(41) Bartlett, P. A.; Spear, K. L.; Jacobsen, N. E. A thioamide substrate of carboxypeptidase A. *Biochemistry* **1982**, *21*, 1608–1611.

(42) Yao, S.; Zutshi, R.; Chmielewski, J. Endothiopeptide inhibitors of HIV-1 protease. *Bioorg. Med. Chem. Lett.* **1998**, *8*, 699–704.

(43) Maziak, L.; Lajoie, G.; Belleau, B. Productive conformation in the bound state and hydrolytic behavior of thiopeptide analogs of angiotensin-converting enzyme substrates. *J. Am. Chem. Soc.* **1986**, *108*, 182–183.

(44) La Cour, T. F. Stereochemistry of peptides containing a thioacyl group. *Int. J. Pept. Protein Res.* **1987**, *30*, 564–571.

(45) Pogorelyi, V. K. Weak hydrogen bonds. *Russ. Chem. Rev.* **1977**, *46*, 316–336.

(46) Pedersen, B. S.; Scheibye, S.; Nilsson, N. H.; Lawesson, S. O. Studies on organophosphorus compounds XX. Syntheses of thioketones. *Bull. Soc. Chim. Belg.* **1978**, *87*, 223–228.

(47) Jesberger, M.; Davis, T. P.; Barner, L. Applications of Lawesson's reagent in organic and organometallic syntheses. *Synthesis* **2003**, 1929–1958.

(48) Bollhagen, R.; Schmiedberger, M.; Kleomenis, B.; Grell, E. A new reagent for the cleavage of fully protected peptides synthesised on 2-chlorotrityl chloride resin. *J. Chem. Soc. Chem. Commun.* **1994**, *29*, 2559–2560.

(49) Gottschalk, M.; Bach, A.; Hansen, J. L.; Krogsgaard-Larsen, P.; Kristensen, A. S.; Strømgaard, K. Detecting protein-protein interactions in living cells: Development of a bioluminescence resonance energy transfer assay to evaluate the PSD-95/NMDA receptor interaction. *Neurochem. Res.* **2009**, *34*, 1729–1737.

(50) Wender, P. A.; Mitchell, D. J.; Pattabiraman, K.; Pelkey, E. T.; Steinman, L.; Rothbard, J. B. The design, synthesis, and evaluation of molecules that enable or enhance cellular uptake: Peptoid molecular transporters. *Proc. Natl. Acad. Sci. U.S.A.* **2000**, *97*, 13003–13008.

(51) Trehin, R.; Merkle, H. P. Chances and pitfalls of cell penetrating peptides for cellular drug delivery. *Eur. J. Pharm. Biopharm.* **2004**, *58*, 209–223.

(52) Delano, W. L. The pymol molecular graphics system on world wide web; http://www.Pymol.Org.

(53) Nikolovska-Coleska, Z.; Wang, R.; Fang, X.; Pan, H.; Tomita, Y.; Li, P.; Roller, P. P.; Krajewski, K.; Saito, N. G.; Stuckey, J. A.; Wang, S. Development and optimization of a binding assay for the XIAP BIR3 domain using fluorescence polarization. *Anal. Biochem.* **2004**, *332*, 261–273.